GEOCHEMICAL AND SEDIMENTOLOGICAL STUDY OF LACUSTRINE SEDIMENTS OF THE *LAGUNA GRANDE*, SOUTHERN SPAIN

GEOCHEMISCHE UND SEDIMENTOLOGISCHE STUDIE AN LAKUSTRINEN SEDIMENTEN DER *LAGUNA GRANDE*, SÜDSPANIEN

Bachelor Thesis

Presented by

Marcel Baum

Matrikelnummer: 319915

Email: marcel.baum@rwth-aachen.de

To achieve the academic grade of Bachelor of Science (B.Sc.) in Georessources Management at the RWTH Aachen University, Neotectonics and Natural Hazards

Summer Term 2015

First examiner:	Univ.-Prof. Dr. Klaus Reicherter
Second examiner:	Dr. Margret Mathes-Schmidt
Supervisor:	M.Sc. Tabea Schröder

Lissabon, 27. September 2015

EIDESSTAATLICHE ERKLÄRUNG

Ich versichere, die Bachelorarbeit selbstständig und lediglich unter Benutzung der angegebenen Quellen und Hilfsmittel verfasst zu haben.

Ich erkläre weiterhin, dass die vorliegende Arbeit noch nicht im Rahmen eines anderen Prüfungsverfahrens eingereicht wurde.

Lissabon, 27. September 2015

ABSTRACT (ENGLISH)

Due to its location in an endorheic basin the Laguna Grande in southern Spain represents a well conserved climate archive for paleoclimatologists to reconstruct the climate of the Holocene of the Iberian Peninsula, particularly in southern Spain. Necessary data were obtained by analyzing drilled lacustrine sediment sequences. Integrated in the C3 project of the Collaborative Research Center 806 “Our Way To Europe” the study focuses on investigations concerning climate anomalies and environmental conditions during the last 190,000 years including the Middle/Upper Pleistocene and the Holocene.

By the conduction of sedimentological and geochemical investiagtions, such as a macroscopical description of the drilling core or CNS and XRF Analysis, the goal was to formulate hypotheses concerning the local and regional climatic and environmental conditions and changes which have influenced the spreading of the Homo sapiens on his way to Central Europe. Obtained data of these investigations including organic matter contents and elemental ratios function as basis for this study.

ABSTRACT (DEUTSCH)

Durch ihre Lage in einem endorheischen Becken repräsentiert die Laguna Grande in Südspanien ein gut erhaltenes Klimaarchiv für Paleolimnologen zur Rekonstruierung des Klimas im Holozän auf der Iberischen Halbinsel, genauer in Südspanien. Die notwendigen Daten wurden mittels Analysen von erbohrten lakustrinen Sedimentabfolgen erhoben. Eingegliedert in den Sonderforschungsbereich 806 „Our Way To Europe“ konzentriert sich diese Studie auf Untersuchungen bezüglich Klimaanomalien und Umweltbedingungen während der letzten 190.000 Jahre, die sowohl das Mittel- und Jungpleistozän, als auch das Holozän umfassen.

Ziel war nach Durchführung von sedimentologischen und geochemischen Untersuchungen, wie einer makroskopischen Bohrkernbeschreibung oder CNS und XRF Analysen, die Formulierung von Hypothesen bezüglich der lokalen und regionalen Klima- und Umweltbedingungen und -veränderungen, die einen erheblichen Einfluss auf die Verbreitung des Homo sapiens auf seinem Weg nach Zentraleuropa hatten. Gewonnene Daten der Untersuchungen, die als Grundlage für diese Studie fungieren, beinhalten unter anderem Anteile organischen Materials und Elementverhältnisse.

ACKNOWLEDGEMENTS

First of all, I would like to thank everyone, who supported and motivated me during my writing of this thesis.

Special thanks goes to Univ.-Prof. Dr. Klaus Reicherter who offered me the possibility to write my thesis in his department of Neotectonics and Natural Hazards and provided me with the necessary equipment.

Another special thank goes to my supervisor Tabea Schröder. From the beginning of the field trip until the end of this thesis she was always available to answer questions, proofread my drafts several times and provided me with information and material for my thesis.

I would also like to thank everyone who was involved in the field trip to southern Spain and the subsequent work in the laboratory in Cologne – Prof. Dr. Martin Melles, Jasmijn van't Hoff, Simon Washausen, Christian Steffens, Daniel Kayser, Florian Steininger, Sandra Jivcov, Raphael Gromig, Ascelina Hasberg, Matthias Thienemann and Dorothea Klinghardt.

Another special thank goes out to the Spanish people who helped us freeing our car while we got stuck in the mud somewhere in Andalusia – gracias por eso!

CONTENTS

LIST OF ILLUSTRATIONS

LIST OF TABLES

GLOSSARY

***Albariza**: Albariza is a type of the Spanish soil classification. It represents a dazzlingly white soil, consists of 40 % limestone as well as clay and sand and its name means 'white earth'.*

***Alboran Sea**: The Alboran Sea is the westernmost portion of the Mediterranean Sea, lying between the Iberian Peninsula and the north of Africa.*

***Alpine orogeny**: The Alpine orogeny is an orogenic phase in the Late Mesozoic and the current Cenozoic that has formed the mountain ranges of the Alpide belt.*

***Cenozoic**: The Cenozoic Era, also known as the Age of Mammals is the current and most recent of the three Phanerozoic geological eras, following the Mesozoic Era and covering the period from 65 million years ago to present day.*

***Dansgaard-Oeschger Event**: Dansgaard–Oeschger events are rapid climate fluctuations that occurred 25 times during the last glacial period.*

***Gondwana**: Gondwana and Laurasia describe the two supercontinents that were part of the supercontinent Pangaea from approximately 300 to 180 million years ago. Gondwana represents in this context the more southerly supercontinent.*

***Heinrich Event**: A Heinrich event is a natural phenomenon in which large armadas of icebergs break off from glaciers and traverse the North Atlantic.*

***Holocene**: The Holocene is the geological epoch that began after the Pleistocene at approximately 11,700 years BP and continues to the present.*

***Middle Weichselian**: The last glacial period and its association glaciation is known in Northern Europe and northern Central Europe as the Weichselian glaciation*

***Piritization**: Piritization describes the process of chemical weathering in which the original substanc e is substituted by pyrite.*

***Pleistocene**: The Pleistocene is the geological epoch which lasted from about 2,588,000 to 11,700 years ago.*

***Quaternary**: The Quaternary Period is the current and most recent of the three periods of the Cenozoic Era in the geologic time scale of the International Commission on Stratigraphy. It follows the Neogene Period and spans from 2.588 ± 0.005 million years ago to the present. The Quaternary Period is divided into two epochs: the Pleistocene and the Holocene.*

***Variscan orogeny**: The Variscan orogeny is a geologic mountain-building event caused by Late Paleozoic continental collision between Laurasia and Gondwana to form the supercontinent of Pangaea.*

LIST OF ABBREVIATIONS

BP - *Before Present*

CNS - *Carbon – Nitrogen – Sulfur*

C/N - *Carbon/Nitrogen*

CRC - *Collaborative Research Center*

ENSO - *El Niño – Southern Oscillation*

IP - *Iberian Peninsula*

MIS - *Marine Isotope Stage*

NAO - *North Atlantic oscillation*

$_{p}CO_{2}$ - *Carbon dioxide partial pressure*

P-E - *Precipitation - Evaporation*

TC - *Total Carbon*

TCD - *Thermal conductivity detector*

TIC - *Total Inorganic Carbon*

TN - *Total Nitrogen*

TOC - *Total Organic Carbon*

TS - *Total Sulfur*

XRF - *X-Ray Fluorescence*

MOTIVATION AND PURPOSE

The climate of the earth is a much-discussed topic in our society. Everyone has heard about major climate events in the past of our planet like the mass-extinction of the dinosaurs caused by a meteorite impact or a volcanic eruption or the Ice Ages when mammoths and saber-tooth tigers walked the earth. All these events were caused by certain climate factors including the sun, the atmosphere with its greenhouse gases, volcanism, continental drifting, the earth's orbit and extraterrestrial factors for example meteorite impacts or solar winds. By using several techniques including the investigation of climate proxies or radiometric dating as well as isotopic signatures scientist are able to reconstruct the paleoclimate and to discover coherences between distinctions or aberrations in their investigations and possible impacts on the climate of the earth.

The reconstruction of the paleoclimate plays a decisive role in geoscience. By analyzing the past in geological periods, variable cycles can be found. Specific repetitions of ice ages or variations in the concentration of gases in our atmosphere are examples for that. Especially the concentration of carbon dioxide is, at present, an important element, particularly with regard to the global warming and the influence of human activity.

All of the aforementioned elements are part of the paleoclimate research, which forms the background of this study – the investigation of lacustrine sediments in southern Spain to reconstruct the paleoclimate of the Iberian Peninsula (IP) over the last Marine Isotopic Stages (MIS).

MOTIVATION

In March 2015, a field trip in cooperation of researchers from the RWTH Aachen University and University of Cologne took place to southern Spain as part of the project 'Our Way to Europe' the name of a Collaborative Research Center of the German Research Foundation. The Institute of Neotectonics and Natural Hazards of the RWTH is part of this project due to the position of Prof. Dr. Reicherter as principal investigator. The task of the field trip was to take samples of several salt lakes in southern Spain and analyze them back home in the laboratories in Aachen and Cologne to contribute to the progress of the project. By using a petrol drill and breaker, we were able to get cores of a length up to around 12 m. Since the quantity and quality of information and data of this region is quite scarce, the results of this field trip are supposed to bring up some completely new findings about the paleoclimate of southern Spain.

This study deals with a geochemical and sedimentological investigation of the drilling cores, which were sampled near the Laguna Grande (Laguna Salada) in the province of Cádiz close to Jerez de la Frontera.

Figure 1 *- Drilling at the Laguna Grande with a vibracorer.*
From left to right: Tabea Schröder, Christian Steffens (kneeling) and Daniel Kayser
(image source: self-made photograph)

PURPOSE

Since this study is part of the project 'Our Way to Europe', the goal is to comprehend how the climate influenced the spreading of the modern human on his way from Africa to Central Europe. Why do we find specific fossils of species of our ancestors in the coastal regions of Andalusia but not further in the interior of Spain? Was the Strait of Gibraltar indeed the way of the modern human to Central Europe? Moreover, if it was, can we find evidence for that to prove this hypothesis?

Viewing the available data and information concerning this issue leads to several conjunctures, which subsequently have to be proven by sampling, analyzing and classifying of the acquired sediment material to gain new findings about the paleoclimate during the time between the Upper Pleistocene and the Middle Holocene of the IP.

Through the cooperation of the geoscientists with archeologists and researchers from other affected science areas, this field trip will hopefully help to bring light in the darkness of the paths of our ancestors (Collaborative Research Center 806, 2009).

INTRODUCTION

THE COLLABORATIVE RESEARCH CENTER 806

The Collaborative Research Center (CRC) 806 of the German Research Foundation also known as the project 'Our Way to Europe' is conducted in cooperation by quaternary researchers from the universities of Cologne (Universität zu Köln), Bonn (Rheinische Friedrich-Wilhelms-Universität Bonn) and Aachen (RWTH Aachen University).

The overall goal of the whole project is to acquire complex chronological, regional-structural, climatic, environmental and sociocultural relations between momentous intercontinental and transcontinental events during the spreading of the modern humans from Africa to Western Eurasia and in particular to Central Europe.

The organization concept of the project is illustrated in the following figure. While the clusters A-D concentrate on the main geographic regions, the clusters E and F deal with integrative and methodological aspects (Collaborative Research Center 806, 2009).

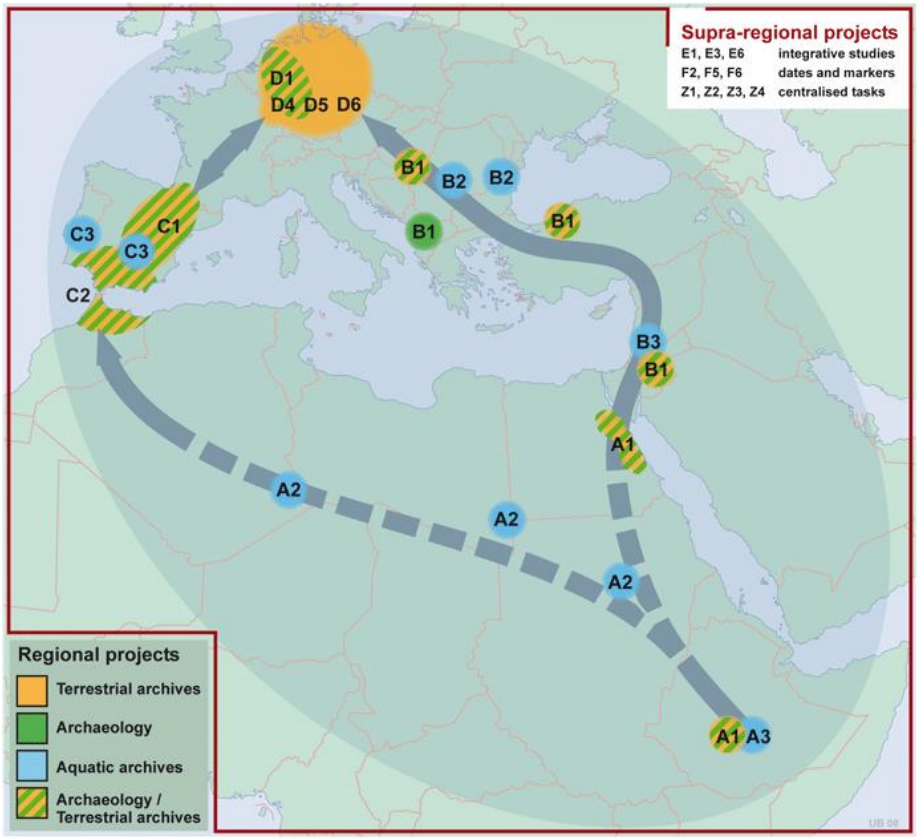

Figure 2 *- Geographical regions of the CRC. The projects A-D are related to specific fieldwork areas, while the E / F projects follow an integrative approach and are displayed in the upper right corner only.*
(Image source: unknown author (internet article): 'Our Way to Europe – Introduction'
URL: http://www.sfb806.uni-koeln.de/index.php/about?showall=1&limitstart=
[Visited: August 17, 2015]

Temporal focus of the project are the last 190,000 years (MIS 1-6) – the time between the spreading of the modern humans from Africa and their settling in Central Europe.

The major themes of the CRC read as follows:

- **First Theme:** The climatic, environmental and cultural context of the primary expansion of the Modern Man, its dispersal from Africa after 190,000 a and the occupation of Europe by 40,000 a.[1]

- **Second theme:** Secondary expansion and retreat of our species, induced by climatic, environmental or cultural changes. For instance the reoccupation of the Near East in the Middle Weichselian and the reoccupation of extensive parts of Europe after the

[1] Cf.: Collaborative Research Center - 'Our Way to Europe – Introduction'
(URL: http://www.sfb806.uni-koeln.de/index.php/about?showall=1&limitstart=)
[Visited: August 17, 2015]

end of the Last Glacial Maximum, which resulted in the spread and establishment of Neolithic economy throughout Europe.[2]

- **Third theme:** Population changes, mobility and migration in coupled cultural and environmental systems, driven by growing impact of human agency on the environment, particularly dispersal, retreat and internal mobility among sedentary prehistoric societies.[3]

There are two main hypothesis concerning the origin of the modern human. The first one is the *Out-of-Africa II* or *Black Eve* hypothesis after which the species Homo Sapiens, our species, has its roots in East Africa (Ethiopia) and spread over the world during the last around 200,000 years while other species including the Homo erectus and the Homo Neanderthalensis coexisted in other parts of Africa, Europe, the Near East and South Asia (**Figure 3**).

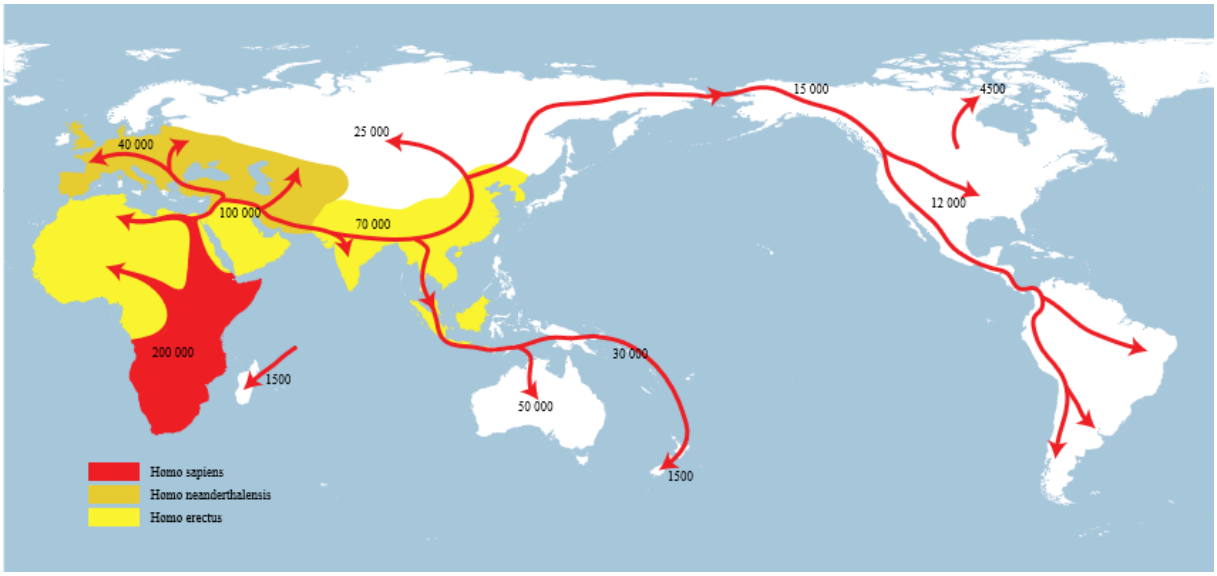

Figure 3 *- Spreading of the Homo sapiens (image source: Wikipedia – 'Mensch' uploaded by user NordNordWest on August 12, 2014)*
URL: https://upload.wikimedia.org/wikipedia/commons/2/27/Spreading_homo_sapiens_la.svg
[Visited: August 18, 2015]

[2] Cf.: Collaborative Research Center - 'Our Way to Europe – Introduction'
(URL: http://www.sfb806.uni-koeln.de/index.php/about?showall=1&limitstart=)
[Visited: August 17, 2015]

[3] Cf.: Collaborative Research Center - 'Our Way to Europe – Introduction'
(URL: http://www.sfb806.uni-koeln.de/index.php/about?showall=1&limitstart=)
[Visited: August 17, 2015]

The second hypothesis which is however supported by only a little minority of the scientists says, that the modern human evolved from several distinct regional branches of the Homo erectus.

In **Figure 2**Fehler! Verweisquelle konnte nicht gefunden werden. and **Figure 4** there are shown two different paths of the modern human to Central Europe. The first one using the eastern corridor is proven, the second one using the western corridor is possible.

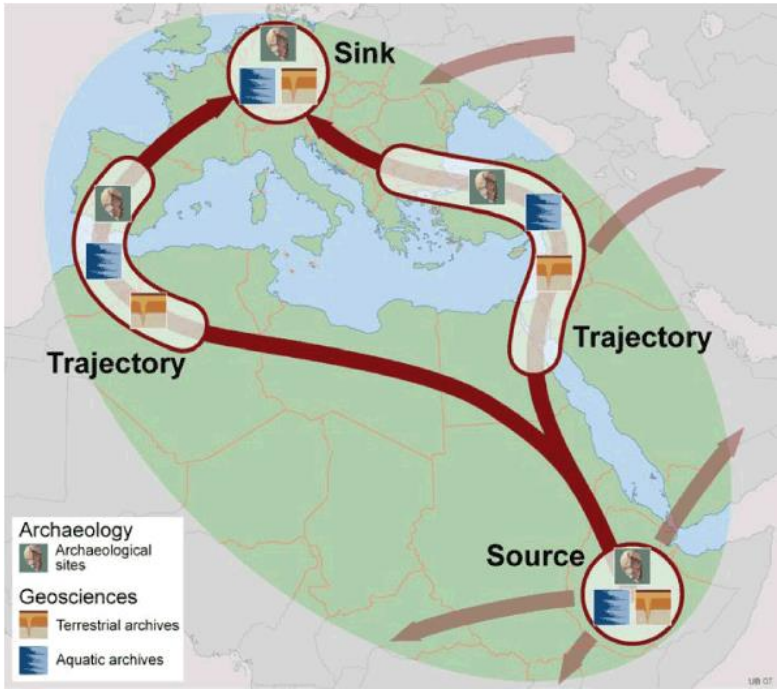

Figure 4 *- Spreading of the modern human with its origin in East Africa (Source), the corridors of diffusion (Trajectory) and settlement in Central Europe (Sink). Object of investigation are archeological, terrestrial and aquatic archives.*
(Image source: unknown author (internet article): 'Our Way to Europe – Introduction'
URL: http://www.sfb806.uni-koeln.de/index.php/about?showall=1&limitstart=
[Visited: August 18, 2015])

As part of the project C3 (**Figure 2**) the responsible region for this study is the IP, particularly the South of Spain with its aquatic and terrestrial archives. The goal is to fill the gap of paleoclimate data of the Late Quaternary between marine records from the Atlantic off Portugal and the Alboran Sea[4] on the one hand and terrestrial records on the IP on the other. This region was inhabited by both Homo neanderthalensis and Homo sapiens and climatically influenced by the North Atlantic Oscillation (NAO), including short-term climate changes like

[4] The Alboran Sea is the most western part of the Mediterranean Sea and located between the IP and the north of Africa. The Strait of Gibraltar connects the Mediterranean with the Atlantic Ocean.

Heinrich Events[5] or Dansgaard-Oeschger Events[6]. The investigations of the C3 project focus temporally on MIS 3 to MIS 2 and thematically on Heinrich and Dansgaard-Oeschger Events since these events forced rapid climate changes, which were accompanied by related movement of the hunter-gatherer populations. As the title of this study says the research concentrates on lacustrine sediments from endorheic 'lagunas' – partly saline or freshwater lakes, which provide long sedimentary sequences. The whole laboratory work on these sediment sequences includes high-resolutional sedimentological, geochemical and geophysical analyses (Multi-Sensor Core Logging, X-Ray Fluorescence (XRF) scanning and organic geochemistry). In cooperation with the cluster F age models will be created based on radiocarbon, luminescence and paleomagnetic dating (Collaborative Research Center 806, 2009).

This study comprises the sedimentological and geochemical part of this analysis with emphasis on XRF and CNS-Analyzes.

PALEOCLIMATE

The term paleoclimate describes the climate of our earth in a geological time scale. Its area of science - the paleoclimatology - addresses the study of changes of the paleoclimate by multi-proxy analyzes. The data for these studies are obtained from natural archives like sediment and ice cores, tree rings, or fossils (shells, corals etc.). Goal of these studies is to reconstruct the climate and determine certain sequences of climate anomalies of this planet in their dependence on terrestrial and extraterrestrial factors to reveal periodicities and make predictions for the climate of the future and possible interactions with anthropogenic influences.

THE CLIMATE OF THE PLEISTOCENE AND HOLOCENE

The climate of the Holocene is characterized by rapid variability, including polar cooling, aridity, and changes in the intensity of atmospheric circulation. These climatic oscillations are recorded in several kinds of cores (polar ice, deep sea etc.). Although it is known for these rapid changes, the climate of the Holocene has been fairly stable since the last ice age.

[5] **Heinrich events** describe natural phenomena in which icebergs break off from glaciers and melt in the North Atlantic. This causes an entry of rock matter (ice rafted debris (IRC)) and cold and fresh water which alters the thermohaline circulation patterns of the ocean (Cacho et al., 1999).
[6] **Dansgaard-Oeschger events** describe rapid climate fluctuations of which 25 occurred in the last glacial period (Cacho et al., 1999).

Nevertheless, because of a lack of agreement about the worldwide distribution, precise timing, amplitude or cause of the fluctuations, investigations of regional records are still necessary.

At a global scale, natural external forcing have been determined as the main influences on climate variability; at a regional scale, patters on natural internal climate variability such as ENSO[7] and NAO[8] are known as oscillating influence on regional climate (Nieto-Moreno et al., 2011).

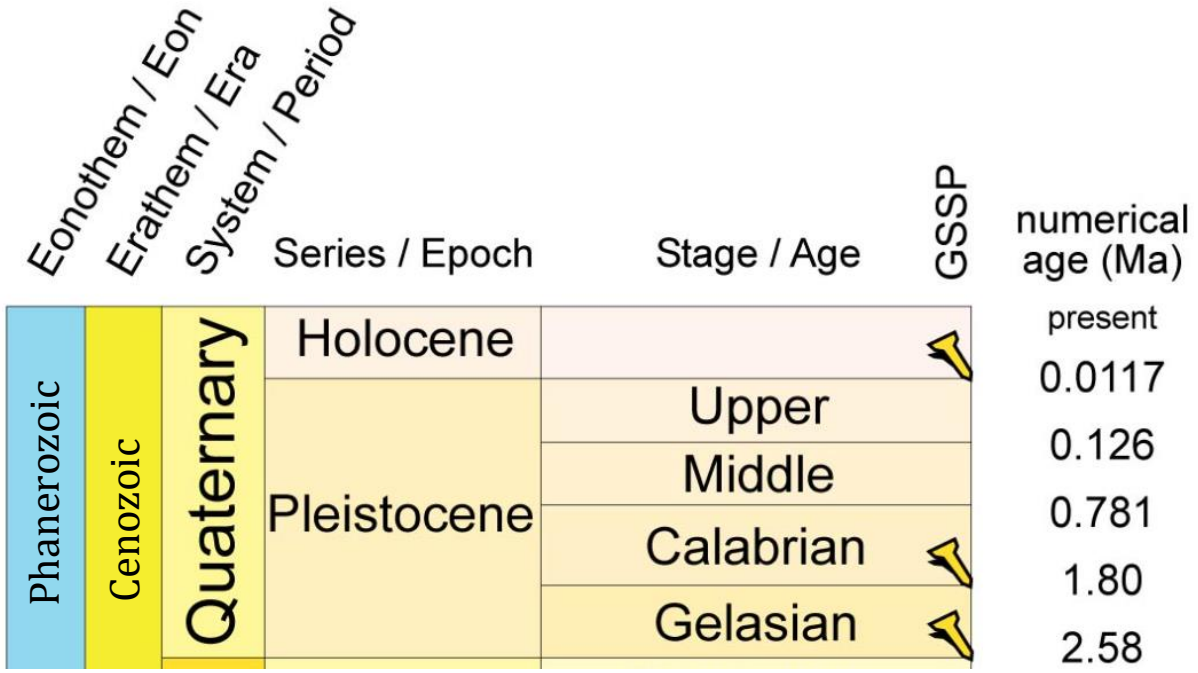

Figure 5 *- Section of the International Chronostratigraphic Chart*
(Image source: International Commission on Stratigraphy
URL: http://www.stratigraphy.org/ICSchart/ChronostratChart2015-01.jpg)

The Holocene as well as the Pleistocene belong to the Quaternary, the youngest system of the Cenozoic. Beginning at approximately 11,700 years BP the Holocene includes also the present. Due to the interaction of the northern Africa subtropical and the midlatitude North Atlantic climate system, the southwestern Mediterranean region is an area of great interest for paleoclimate research. By controlling the climate variability of this region as of the mid Holocene these two influences are the reason for the unique environmental conditions that determine the landscape as well as biota and human society's evolution. The Mediterranean

[7] ENSO : El Niño-Southern Oscillation
[8] NAO : North Atlantic Oscillation

region is characterized by semi-humid Mediterranean climate with warm and dry summers and mild an wet winters (Martín-Puertas, 2010).

PALEOLIMNOLOGY

Lake systems are considered valuable archives for climate reconstruction. Since they are sensitive towards climate changes their responses are usually physically, chemically and biologically registered and manifested in sediment records. In closed lake basins like the Laguna Grande change of water level can for example lead to significant changes in salinity and ionic composition. These different levels of salinity and ionic composition are reflected in composition and ratios of fossils and elements in the sediment layers. Since temperature changes influence the lake level significantly, a reconstruction of the climate is possible by analyzing drilling cores. A multi-proxy analysis of the effects of temperature changes on nutrient cycling, alkalinity generation, water column stratification and fossil composition and an understanding of the processes that are operating in the water column are considered the best way to achieve accurate results of climate reconstruction (Battarbee, 2000).

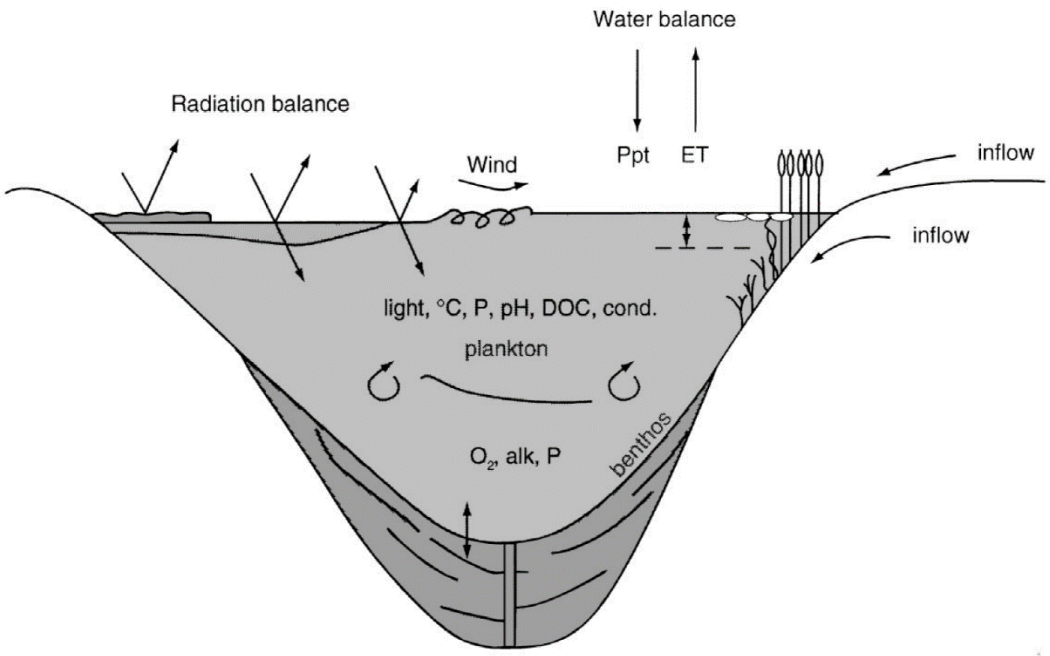

Figure 6 *- Schematic diagram to show examples of the principal physical, chemical and biological responses of lake systems to changes in climate forcing.*
(Image source: Battarbee, R. W., 2000. Palaeolimnological approaches to climate change, with special regard to the biological record)

The main use of paleolimnological methods consists in effective moisture (precipitation and evaporation (P-E)) and temperature. Nevertheless scientists attempted as well to to relate sediment records to wind regimes, moisture sources, atmospheric circulation patterns and atmospheric $_pCO_2$. By using results from direct observations from instrumental records to compare them with results from a multi-proxy paleolimnological analysis, a separation of the influences of temperature, moisture or wind regimes is rather possible since the individual effects are quite difficult to determine by only using the proxy data (Battarbee, 2000).

Probably the best type of lake for paleolimnological analysis are closed-basin salt lakes (Laguna Grande). They are located in semi-arid or arid regions and have little or no outflow (surface or groundwater) which makes them hydrologically closed (permanently or periodically). Moisture losses are dominated by evaporation. Lakes of this type used to have a high ionic concentration. Already small changes in P-E can result in significant lake-level and salinity variations recorded in the sediments. Lakes which have a reasonable depth, sufficient for sediments to have accumulated continuously even during the driest periods, are the most suitable ones for paleolimnological investigations (Battarbee, 2000).

GEOGRAPHY OF SPAIN AND THE PROVINCE OF CÁDIZ

With 505,992 km^2 Spain is the fifty-second largest country in the world and the fourth largest country in Europe. The Pico del Teide on Tenerife is with 3,718 m the highest mountain peak in Spain (Central Intelligence Agency, 2014) and also the third largest volcano in the world.

Spain lies between latitudes 26° and 44° N, and longitudes 19° W and 5° E.

With Portugal, France, Andorra and Gibraltar Spain forms the Iberian Peninsula and covers around 85 % of its area.

Spains land boundaries have a length of 1,952.7 km. On the west, it borders Portugal, on the south Gibraltar (British overseas territory) and Morocco through its exclaves in North Africa (Ceuta, Melilla, Vélez de la Gomera) and on the northeast, along the Pyrenees mountain range, it borders France and the Principality of Andorra.

Figure 7 *- The topography of Spain (Image source: Virgil Interactive GmbH, worldofmaps.net (internet page) URL: http://www.worldofmaps.net/en/europe/map-spain/topographic-map-spain.htm [Visited: September 6, 2015]*

Cádiz is a province of southern Spain in the southwestern part of the autonomous community of Andalusia and has an area of 7,385 km^2.

It is bordered by the Spanish provinces of Huelva, Seville, and Málaga, as well as by the Atlantic Ocean, the Mediterranean Sea, the Strait of Gibraltar and the British overseas territory of Gibraltar.

Its capital is the city of Cádiz, which has a population of more than 128,000. The largest city is Jerez de la Frontera (Central Intelligence Agency, 2014).

Figure 8 *- Spain with its administrative divisions (Image source: Virgil Interactive GmbH, worldofmaps.net (internet page)*
URL: http://www.worldofmaps.net/en/europe/map-spain/map-administrative-divisions-spain.htm
[Visited: September 6, 2015]

GEOLOGY OF THE IBERIAN PENINSULA

The geology of the Iberian Peninsula comprises an outstanding diversity of rock formations. Remarkable are especially the Paleozoic sedimentary sequences which are one of the most complete ones in Europe. Moreover, it includes a distinguished record of the effects of the Variscan orogeny on the margins of Gondwana, the former supercontinent. Spains present geomorphology has been mainly created by Cenozoic events linked to the Alpine orogeny. Located between the African and the Eurasian continental plates, Spain is bordered by two big mountain chains. While the northern border is formed by the Pyrenees-Basque-Cantabria belt, the southern border is formed by the Betic Cordilleras. Due to Alpine collision Pyrenean Iberia became partly subducted beneath the Eurasian plate whereas in the south Ibero-African collisions produced the Betics. Both of these zones have generated typical foreland basins, the Ebro basin south of the Pyrenees and the Guadalquivir basin in the north of the Betics. The core of the Iberian Peninsula is dominated by two large Cenozoic basins drained by the Tajo river in the south and the Duero river in the north (**Figure 9**). These basins form high but relatively flat areas which are called 'mesetas'. The granite-dominated highlands of the Central Range separates these areas. (Gibbons & Moreno, 2002).

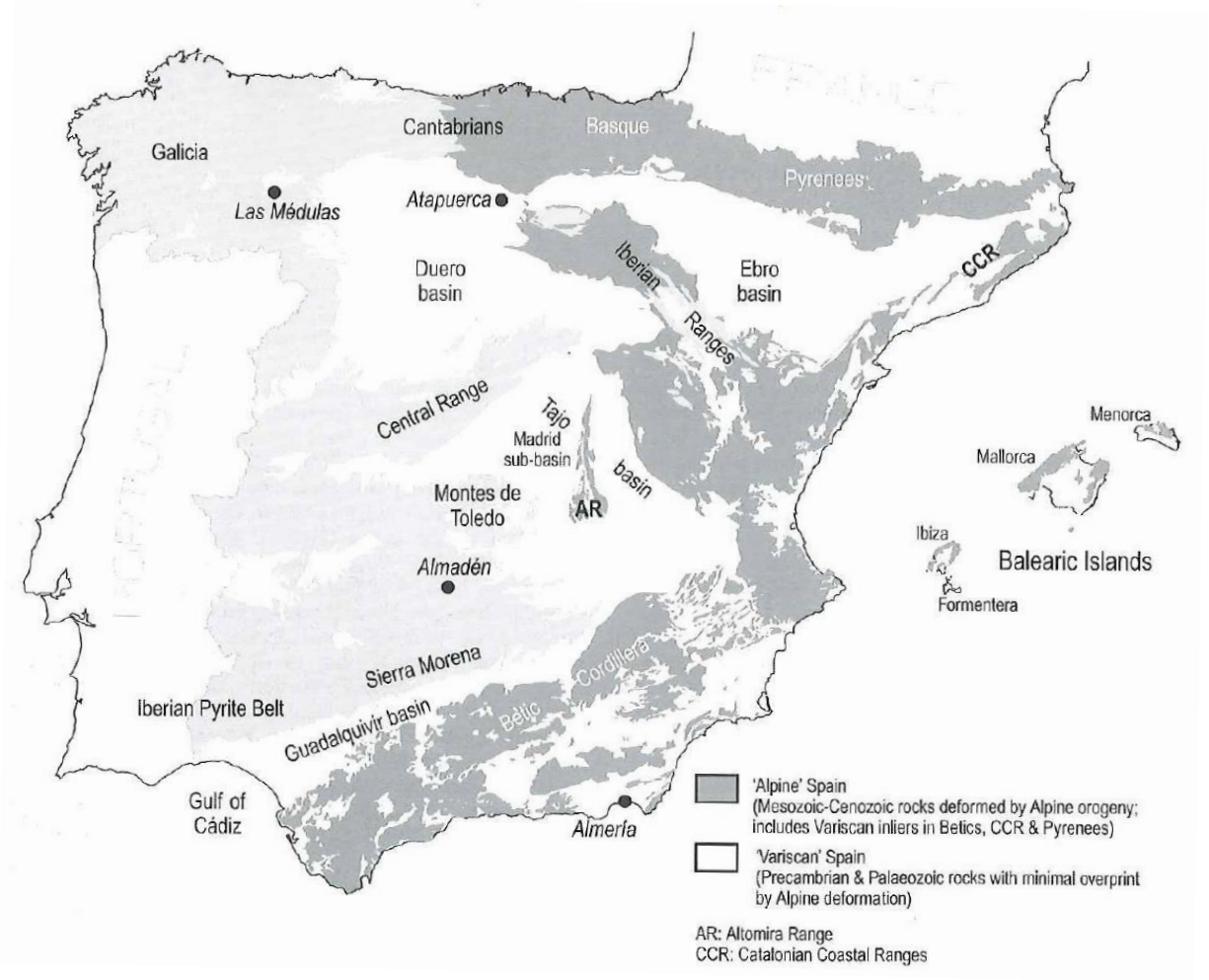

Figure 9 *- Outline map of mainland Spain showing the broad division into 'Variscan' and 'Alpine' Spain. White areas in Spain are Canozoic basins.*
(Image source: Gibbons, W., Moreno, T., 2002. The Geology of Spain, The Geological Society London)

SIERRA MORENA

The Sierra Morena forms the southern border of the Iberian Massif and is one of the main systems of mountain ranges in Spain. It stretches for 450 kilometers from east to west across the south of the Iberian Peninsula and is the result of the uplift along the Guadalquivir basin produced by the pressure of the northward-moving African Plate during the Alpine orogeny. It comprises Precambrian and Paleozoic rocks, which are partly metamorphic altered such as granite and quartzite and softer materials such as slate and gneiss (Gibbons & Moreno, 2002).

The peaks of the ranges are not very high. The highest point is the lowest among the mountain systems of the Iberian Peninsula. However, they are very consistent in altitude, averaging between 600 and 1,300 m all along the system (Gibbons & Moreno, 2002).

BETIC CORDILLERA

The Betic System (Spanish: Sistema Bético) is one of the main systems of mountain ranges in Spain and is located in the south and southeast of the Iberian Peninsula.

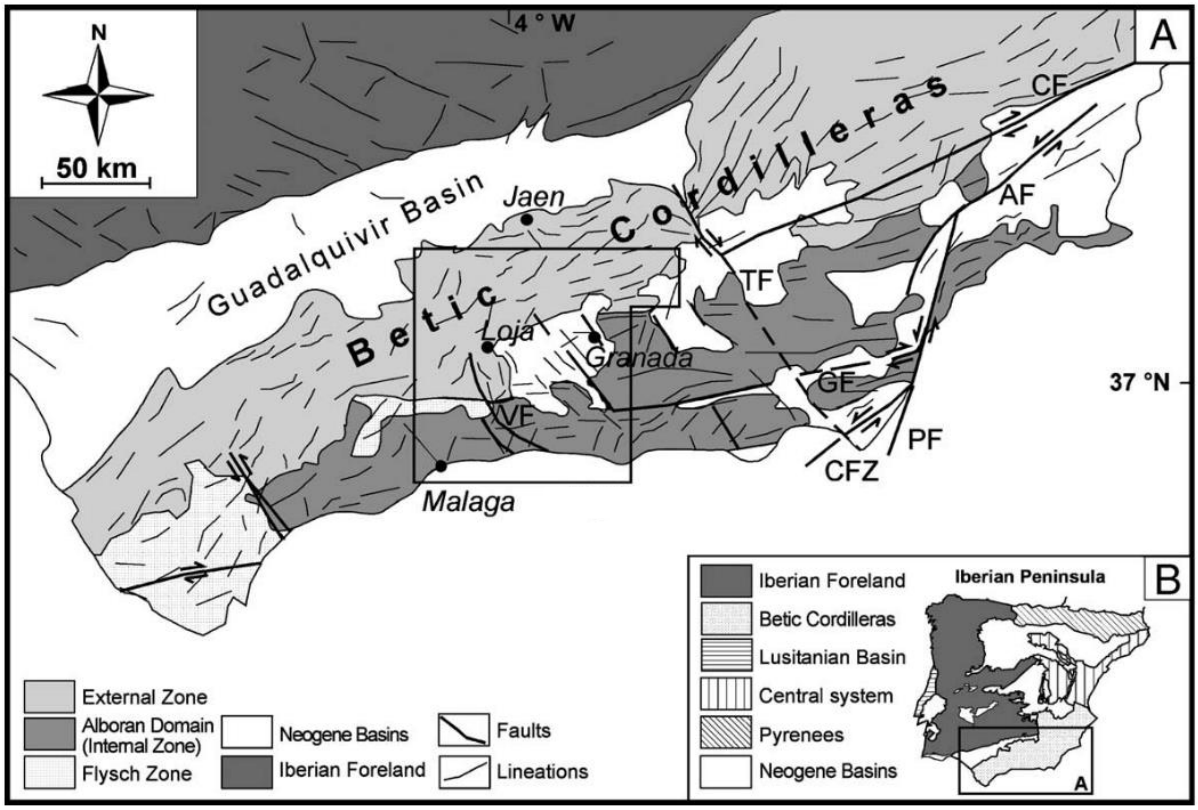

Figure 10 *- The Geology of southern Spain*
(Image source: Reicherter, K. R., Peters, G., 2004. Neotectonic evolution of the Central Betic Cordilleras (Southern Spain))

They form the northern part of the Gibraltar Arc which represents the westernmost edge of the Alpine orogenic system and continue in the Rif in Morocco in the southwest of the Iberian Peninsula and in the Balearic Islands in the northeast. The Betic Cordillera is traditionally divided in two main domains; the Alboran Domain (Internal Zones) on the one hand and the South Iberian Domain (External Zone) on the other hand (González-castillo, Galindo-zaldívar, Junge, Martínez-moreno, & Löwer, 2015). A series of nappes of marine sediments (Flysch Units) occur along the contact between the External and the Internal Zones (Gibbons & Moreno, 2002).

Defined is the tectonic framework of the Iberian subplate by the continuing convergence of Africa as of the Late Cretaceous. Since the Betic Cordilleras are located in this region, the

structure of the Betic orogen is caused by the oblique convergence and collision of the Iberian and African plate initiating in the Santonian/Campanian (about 86.3 mya). Due to these collisions metamorphism and thrusting took place within the Alboran Domain (Reicherter & Peters, 2005). The Sierra Nevada, which also comprises the highest mountain peak of the Spanish mainland, forms the center of the mountain chain, which stretches over more than 600 km from the Bay of Cadíz to the region of Valencia (Gibbons & Moreno, 2002).

Cenozoic Basins/ Guadalquivir Basin

The Neogene Guadalquivir Basin is a large flexural foreland basin with a linear ENE-WSW trending. It's bordered to the north by the Iberian Massif and to the south by the Betic Cordillera and filled with a middle Miocene sedimentary sequence (Serrano, Torcal, & Benito, 2015). Like any other Neogene basin it developed and filled while the Betic mountains uplifted. It shows an asymmetrical geometry with sediment thickness increasing southeastwards (Gibbons & Moreno, 2002).

SEDIMENTOLOGY AND GEOCHEMISTRY

Research in fields like the CRC 806 requires a complex and eclectic workflow. The entirety of all disciplines lead to a result based on many independent studies. Since this thesis addresses the sedimentological and geochemical part of the project this chapter is supposed to give a brief introduction into the applied types of analyzes which are later explicitly explained in chapter 5 and 6.

In sedimentological analyzes the drilling core gets investigated macroscopically. Determination of grain size, classification of the type of soil and a description of color, structure and bioturbation are the main objects of investigation. Geochemistry offers a wide range of different types of analyzes such as CNS-Analyzes, XRF-Scanning, TIC/TOC-ratios, Isotope ratios and much more. So basically all processes with chemical, physical or biological character are included in this term. Goal of the multi-proxy analyzes conducted by the CRC 806 is always to discover differences or anomalies and draw conclusions about these observation concerning environmental conditions like ice ages, floods, droughts or other climatic distinctions like Heinrich Events or Dansgaard-Oeschger Events.

STUDY AREA

LOCAL GEOGRAPHY

The study area is located in the province of Cádiz in the southwest of Andalusia, an autonomous community of the Kingdom of Spain. The nearest cities are El Puerto de Santa María (5 km), Jerez de la Frontera (about 10 km) and Cádiz (15 km). Main object of investigation is the Laguna Salada or Laguna Grande which is part of the natural reserve named Complejo Endoreico del Puerto de Santa María. This natural reserve is less than 10 km away from the coast of the Atlantic Ocean and the river Guadalete. Climatically this regions is classified as semi-arid which means, that the precipitation exceeds the value of evaporation in three to five months per year (Podbregar, Schwanke, & Frater, 2009).

During the field trips to the Laguna, five drillings were conducted. The cores with the names LSL 1 and LSL 2 were gathered in September 2014 in the middle of the lake while it was dried out caused by poor precipitation. The cores LSL 3 to 5 were sampled in March 2015 at the

bank of the Laguna since it was flooded (**Figure 13**). This study focuses on the cores LSL 1/2 with the coordinates: *36°38'37.4" N, 006°14'09.0" W*

The maximum depth is 11.7 m while the second core was drilled with an offset of 0.5 m. Thus the cores overlap with a difference of 0.5 m which promises enhanced results after correlation.

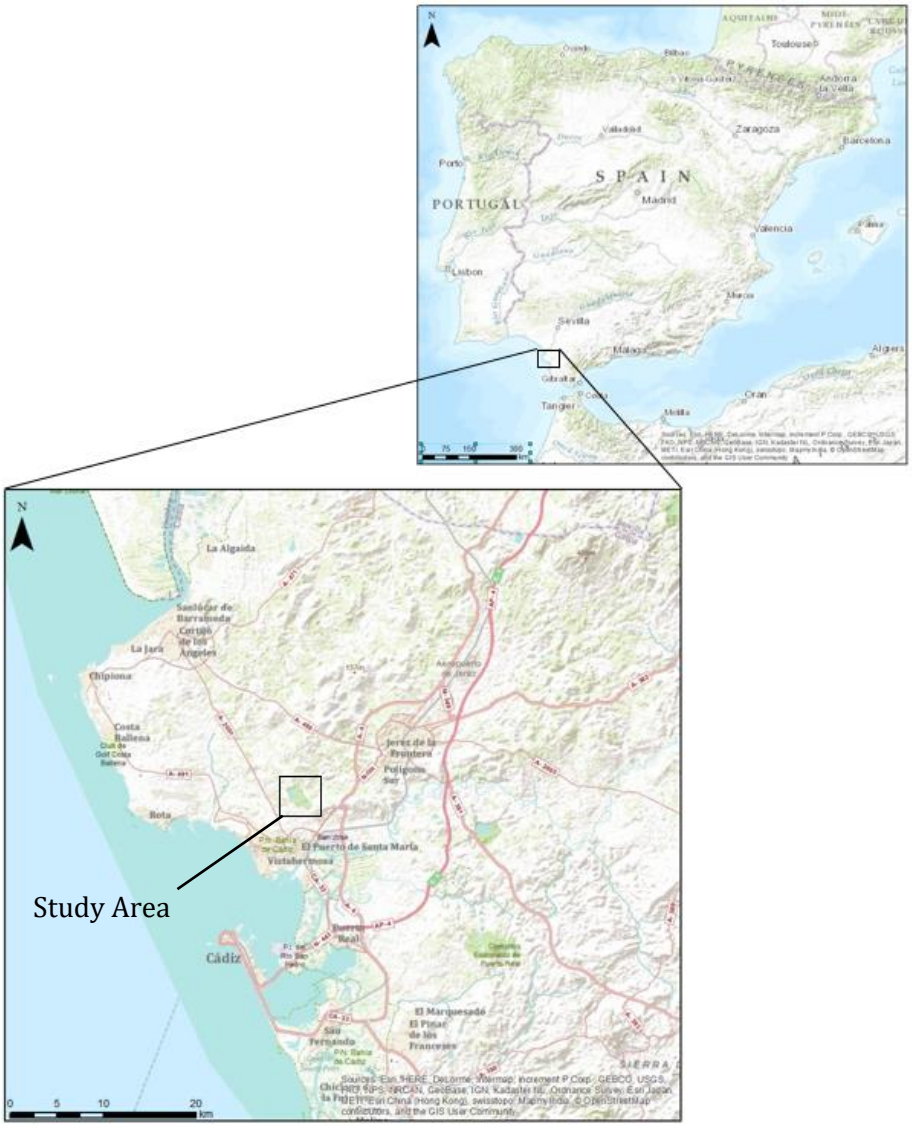

Figure 11 *- Geographic position of the study area on the Iberian Peninsula (Image source: ArcGIS)*

LOCAL GEOLOGY

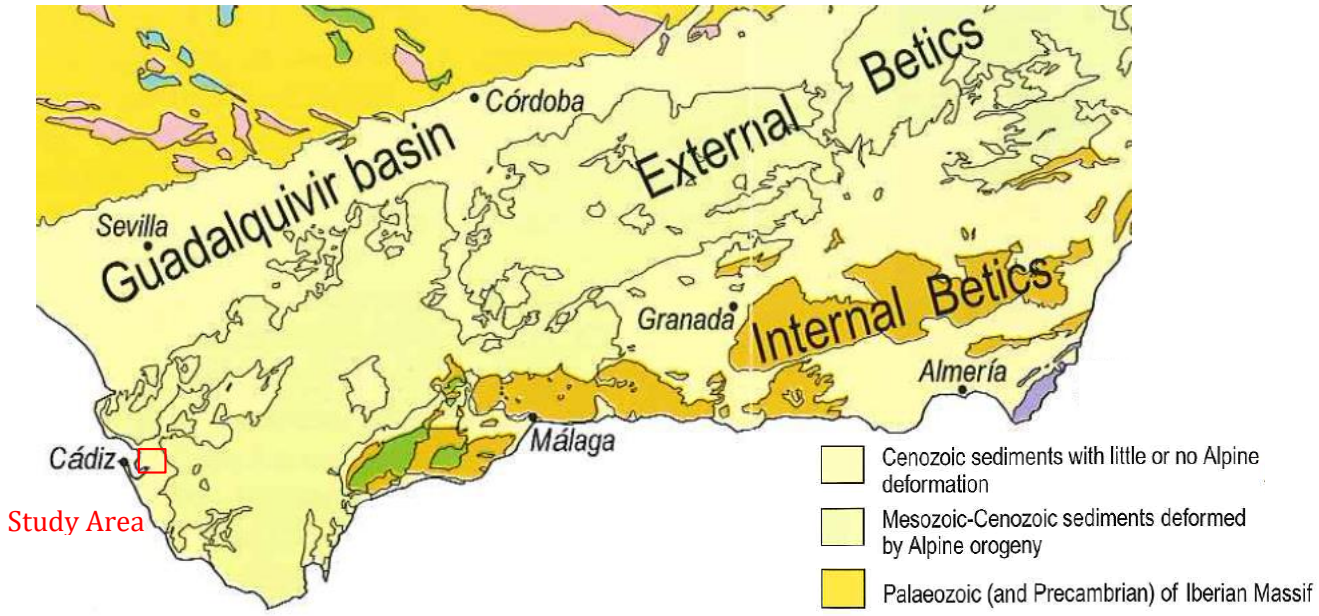

Figure 12 *- Geology around the study area*
(Image source: Gibbons, W., Moreno, T., 2002. The Geology of Spain)

With its location in the Guadalquivir Basin (**Figure 12**), the study area has quite an interesting geological history. The main geomorphology of Andalusia is very mountainous due to the Betics. It is crossed by several small areas of Cenozoic basins and includes the big Guadalquivir basin in the north of the Betics. The study area is located in the border zone of the basin and the Betics and is relatively flat in comparison to the region further in the mainland. The material of the basins consists mainly of Neogene to Quaternary sediments (Reicherter & Peters, 2005).

SALT LAKES OF SOUTHERN SPAIN

There are approximately 2,500 lakes in Spain of which around 80 are inland salt lakes. Due to the arid conditions in the Spanish endorheic areas most lakes are temporary. In general the Spanish salt lakes are divided into four main district: The Ebro river basin, the Northern Castile Tableland, the Southern Castile Tableland and Southern Spain. Most of the lake basins in Spain were formed in karstic areas by hydrologic and Aeolian erosions.

The existing 4 main types of Spanish salt lakes are:

- Temporarily mineralized but not highly saline (salinity < 7 g/l
- Temporary salt lakes with fluctuating salinity (salinity from 7 to 300 g/l)
- Permanent salt lakes

In 1940, *Dantin* listed 17 salt lakes in southern Spain which are all located close to the Guadalquivir river. Laguna Grande, the object of this thesis is one of them. While several of these lakes were and are desiccated for agriculture the Laguna Grande is spared from these influences due to its location in the natural reserve.

The chemistry of the Spanish salt lakes is characterized by a large amount of sodium-chloride and magnesium sulphate. The reason for that are the sedimentary rocks which form the Tertiary evaporitic basins of the lake systems. Gypsum ($Ca[SO_4]\cdot 2H_2O$), marls and limestones ($CaCO_3$) are the main rocks fround in the basins (Comin & Alonso, 1988).

LAGUNA SALADA/GRANDE

THE COMPLEJO ENDORREICO DE EL PUERTO DE SANTA MARÍA

The natural reserve Complejo Endorreico de El Puerto de Santa María is located in southern Spain close to Jerez de la Frontera and comprises three lakes. The Laguna Salada, Chica and Juncosa (**Figure 13**) represent a valuable milieu for several species of birds and plants. The name already describes the environmental conditions. An endorheic basin is a closed drainage basin. The water retains in the basin and there is no outflow into the sea. Differences in water level are caused by rainfall and evaporation which causes a relatively high level of salinity (Iacobellis, Castorani, Rosario, Santo, & Gioia, 2015). The endorheic complex is geomorphologically characterised by a rather gentle topography. Predominant materials which form the basis of the complex are white, silty and marly Albarizas[9] (Junta de Andalucia, 2003).

[9] La Albariza is a Spanish type of soil classification.

Figure 13 *- The Complejo endorreico de El Puerto de Santa María with its three lakes Laguna Salada, Chica and Juncosa and the drilling spots (Image source: ArcGIS).*

Coordinates of drilling spots:

LSL 1&2:	*36°38'37.4'' N, 006°14'09.0'' W*
LSL 3:	*36°38'36.0'' N, 006°14'01.6'' W*
LSL4:	*36°38'57.5'' N, 006°14'01.1'' W*

LA LAGUNA SALADA/GRANDE

The Laguna Salada with a surface area of around 27 ha represents the largest lake of this complex. This fact apparently also leads to its second name, the Laguna Grande which was also used in this thesis. It has a watershed area of 157.45 ha and the maximum depth amounts more than 2 m. In years of high rainfall the Lagunas Salada and Chica remain flooded while in years of average (595 mm[10]) or substandard rainfall they dry out during the summer months. However, the Laguna Juncosa is clearly just temporary flooded (Junta de Andalucia, 2003).

The salt concentration of the Laguna Salada is slightly higher than the one of the Laguna Chica which is probably caused by clay-gypsum materials cutting the overlying materials. This leads to a lower dissolving capacity. The salinity itself fluctuates widely over the years. While in

[10] Data from Climate-Data.org (URL: http://es.climate-data.org/location/56991/)

1997/98 the recorded values were ranging between 0.8 g/l and 2.2 g/l, in 2003 the salinity reached values of 15 g/l (**Figure 14**) (Junta de Andalucia, 2003).

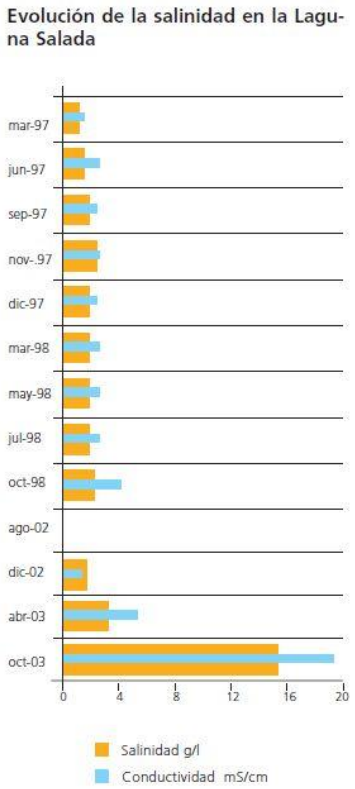

Figure 14 *- Salinity (orange) and conductivity (blue) of the Laguna Salada in 1997/98 and 2002/03 (Image source: Junta de Andalucia, Lagunas Salada, Chica y Juncosa URL: http://www.juntadeandalucia.es/medioambiente/web/Bloques_Tematicos/Estado_Y_Calidad_De_Los_Recursos_Naturales/Ecosistemas/Humedales/03_salada.pdf [Visited: September 16, 2015]*

The water is alkaline with a pH ranging between 7.4 and 9.3 and it comprises a moderate chlorophyll content with a maximum measured rate of 15 mg/m³. The ionic composition is dominated by Na+, Cl-, SO42- and Ca2+ (Junta de Andalucia, 2003).

METHODS IN THE FIELD

VIBRACORER

The main method in the field is the application of the vibracorer, a technique which was developed for investigations in marine coastal and shelf oceanographic milieus. Due to its ease of operation and portability it became increasingly popular under paleolimnologists for collecting cores with a maximum length of 15 m in unconsolidated sediments. The common use of vibracorers is quite simple. A combustion engine driven vibrator and a core tube form

the two main components of the machine. The vibrator transmits high-frequency, low amplitude standing waves along the length of the tube. At the end of the core tube a thin layer of water-saturated sediment gets liquefied by these vibrations. Due to the resulting loss of solidity the core tube is able to penetrate forward through the sediment easily. An additional and manual application of vertical force is (almost) not necessary.

Although vibracorers captivate due to their simple operation and construction, high mobility, low cost in production, versatility and fast work processes, there are also disadvantages. The most common ones are poor velocity in penetration and recovery in some types of sediment and compaction.

Additionally the fall-back while obtaining the actual sediment core from the borehole remains a problem. The core tubes we used all had a length of 1 m which implicates, that they had to be extended after every 1 m of drilling. Therefore, the vibrator were taken off from the tube and a hydraulic puller was applied to get the tube out of the hole. Subsequently, the drill string got extended by another meter and placed back. The intensity of the fall-back problem, which occurs during this process of pulling out the tube, depends on the sediment. In more aqueous and finer sediments a comparable bigger amount of sediment (fall-back) falls on the ground of the borehole from the perimeter. This problem occurred mainly at the shore drillings (LSL 3, 4, 5) whereas the sampling of LSL 1 and 2 was less affected by this problem due to drier sediments.

To still get a continuous and undisturbed sequence of sediment the base of the tube first has to be returned on the initial depth before every drilling process. The sampled fall-back can be removed through an orifice on top of the tube. Furthermore, a second drilling is conducted to improve the results. By changing the points of depth the drill string gets extended, disturbed sequences of the first core can be fixed through correlation with the second core (Last & Smol, 2001a).

METHODS IN THE LABORATORY

MACROSCOPIC DESCRIPTION OF THE DRILL CORE

Once the drilling cores were sampled the liners[11] were cut into pieces, each with a length of 1 m and sealed. After the field trip and the transport to the laboratory the liners were stored in a cooling chamber at 4 degrees Celsius protected against sunlight.

The subsequent analysis started with a macroscopic description of each core. Therefore, the liners were opened vertically with a circular saw and afterwards horizontally with a wire cord. The result were two half shells of the liner of which one was used for further analysis while the other one was stored again. There are several different ways how to describe a drilling core macroscopically. For this analysis we chose the one after Martin Kehl (**Appendix**), a professor of the Geographic Institute of the University Cologne. His guide contains the following items:

1. **Consecutive numbering** of the sequences of the core (sequences have varying lengths)
2. **Lower layer boundary** with depth and art of junction
3. **Color** determined in moist status by using the Munsell color system of the following color components
    a. Hue
    b. Value
    c. Chroma
4. **Mottling and stratification** (area and size)
5. **Moistness** (dry, moist, wet, water saturated)
6. **Soil type** (by using identification keys)
7. **Coarse amount** (amount of gravel and culm)
8. **Carbonate contents** (intensity and duration of the reaction with hydrochloric acid)
9. **Organic matter** (estimations by using the soil color of a moist sample)
10. **Bedding** (bulk density)

[11] A liner is another tube, in this case out of plastic, inside the metal drill string. It contains the sediment core and is used for transport, protection, conservation and storage.

11. **Concentrations** of clay, secondary carbonates, gypsum crystals, iron and manganese hydroxides)
12. **Remarks**

CNS ANALYSIS

To keep on working and analyzing, the sediment core in the liners got sampled every 6 cm. After a measurement of the samples wet weight they were frozen for at least 24 h at –20 degrees Celsius and afterwards freeze-dried for 72 h. Subsequently, they were measured again to ascertain their dry weight, respectively their water content. The resulting samples were grinded to a particle size comparable to silt (0.002 – 0.063 mm) by using agate mortars. To measure the amount of Carbonate, Nitrogen and Sulfur in organic and inorganic compounds 5 mg of each sample (180 in total) were mixed together with 20 mg of tungsten trioxide to ensure a complete combustion in little tin boats. Afterwards, the tin boats were folded to avoid loss of the mixture and listed to keep an overview. Additionally after every ten samples two standards were mixed with the tungsten trioxide to avoid errors in measurement. These two standards[12] have known values for C, N and S. The prepared samples were put into the vario MICRO cube, a micro-analyzer with simultaneous CHNS determination (**Figure 15**).

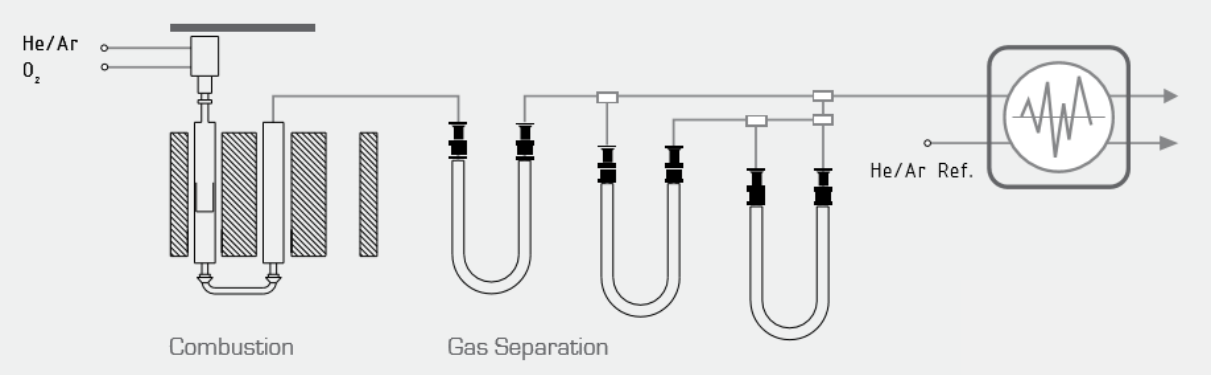

Figure 15 *- Process of the CNS Analysis showing the combustion, separation and detection (Image source: vario MACRO cube manual URL: http://www.vertex.es/portal/docs/elementar/C_Elementar_vario_MACRO_cube.pdf) [Visited: September 22, 2015]*

[12] The used standards were called LKSD-3 and EM-4

In the analyzer, the samples were transferred automatically through the ball valve into the combustion tube. Here they were flushed with helium carrier gas to remove atmospheric nitrogen before the catalytic combustion starts at a temperature of up to 1,200 °C. In the following reduction tube the combustion gases were reduced on hot copper. The resulting analyte gas mixture N_2, CO_2, H_2O and SO_2 remain in the helium carrier gas stream and get separated via purge & trap chromatography and detected by a thermal conductivity detector (TCD). A connected PC finally computed the element concentrations from detector signals and the sample weights (Elementar Analysensysteme GmbH, n.d.).

X-RAY FLUORESCENCE (XRF)

Besides the CNS Analysis this thesis also addresses X-ray fluorescence analysis. The term X-ray fluorescence (XRF) describes the emission of photoelectric fluorescence or secondary x-rays from samples, which were stimulated by irradiation with suitable primary photons. These primary photons are provided by radioisotopes in isotope source systems or, in tube source instruments, generated by accelerating electrons onto a suitable target in the tube (Last & Smol, 2001b).

In simplified terms, the energies of the secondary X-rays are related to the specific elements and the rate of emission is roughly a function of their concentration and adsorption of the outgoing X-rays by the sample.

The underlying physics is a bit more complex though. If an atom is exposed to these X-rays, which have an energy higher than the ionization potentials of the atoms, it emits one or more electrons. The ejection of electrons involves also a destabilization of the electronic structure of the atom. Due to the loss of electrons, gaps emerge in random orbitals. Now, electrons from higher orbitals tend to fill these gaps. During this process of ‘falling down’ energy (equal to the energy difference of the two orbitals) is released in form of a photon. Hence, the sample emits radiation with a characteristic energy of the involved atoms. The term fluorescence signifies in this context the re-emission of radiation of a different energy (generally lower) due to its absorbed radiation. Since the re-emitted energy has a longer wave length it can also occur in the ultraviolet region of the spectrum and is thus visible to the human eye when exposed to UV light (Last & Smol, 2001b)(Croudace, 2006).

The next step of analyzing is now the connection between specific elements and their characteristic radiation due to their diversity of electronic orbitals. The wave length, which is associated with the energy emitted by the transition, can be calculated with Planck's Law.

Once the different wave lengths are sorted and related to specific elements, the XRF Analysis is a powerful tool to determine the elements included in the sample.

These elemental ratios get interpreted later and act as an indicator for specific environmental conditions (Last & Smol, 2001b)(Croudace, 2006).

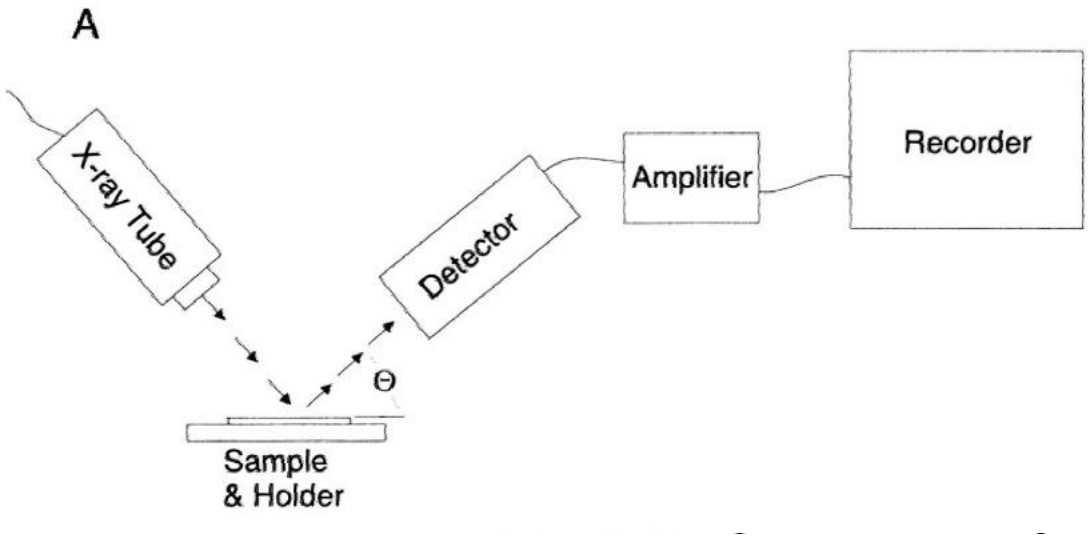

Figure 16 *- Schematic diagram showing the process of X-ray diffraction analysis*
(Image source: Last, W., Smol, J., 2001. Tracking Environmental Change Using Lake Sediments. Volume 2: Physical and Geochemical Methods)

RESULTS

MACROSCOPIC DESCRIPTION OF THE DRILL CORE

The two drilling cores LSL1 and LSL2, which were correlated to obtain optimal results, display a sedimentary sequence with a length of 11.7 m. However, the sequence contains gaps without any information in the following depths:

- 0.61 m – 0.64 m
- 0.95 m – 1.00 m
- 1.98 m – 2.00 m
- 3.99 m – 4.02 m
- 4.54 m – 5.00 m
- 5.78 m – 7.00 m
- 7.98 m – 8.00 m
- 8.63 m – 9.00 m

For the macroscopic description of the sedimentary sequence the guideline of Martin Kehl was used as explained in (**Appendix**) and the results were documented in the following table:

Table 1 *- Results of the macroscopic analysis of the drilling core*

Name of the drilling core	from (cm)	to (cm)	Soil type	Color	Lower layer boundary	Mottling, stratification	Moistness	Coarse amount	Carbonate contents	Org. matter	Notes
LSL1	0	13	Tt	5Y 3/1	A	V, MG	F	0	c1/c2	h3	
LSL1	13	61	Tt	5Y 5/1		W, F	F	0	c2	h1	18-23: Grüne Flecken GLEY 1 4/56 23-30: Gelbe Flecken 2,5Y 4/3 39-42: Weiße Gipsflecken 42-61: Gelbe Flecken 2,5Y 4/3 25cm Organic 49cm Schalenreste
LSL2	64	93	Tt	5Y 5/1	De	W, F	F	0	c3	h1	Gelbgrüne Flecken (5Y 5/6) 76: Gips, wenige Schalenfragmente
LSL2	93	95	Tt	2,5Y 6/3		W, F	F	0	c2	h1	Heller Ton
LSL1	100	130	Tt	5Y 4/1	Di	S, F	F	0	c2	h2	Ab 120cm wenige kleine Gipsstücke
LSL1	130	149	Tt	5Y 5/2	De	V, G	F	0	c2	h1	138-151: kleine grün/gelbe Flecken und weiße Gipsflecken
LSL1	149	152	Tt	5Y 3/2			F	0	c3	h3	Weiße Gipsflecken
LSL2	152	165	Tt	2,5Y 3/1 2,5/1	Di	SV, G Dunkle Flecken, helle Matrix	F	0	c3	h3	Bioturbation Gipskristalle

LSL2	165	198	Tt	2,5Y 4/1		SV, G W, MG	F	0	c2	h2	Immer weniger Flecken Gipskristalle
LSL1	200	220	Tt	5Y 4/1	Di	SV, G	F	0	c2	h2	Überall Schalenfragmente
LSL1	220	250	Tt	5Y 5/2		SV, MG	F	0	c2	h1	Weniger Schalenfragmente
LSL2	250	277	Tt	2,5Y 6/2	Di	V, G immer weniger	F	1, gr	c3	h1	260: Schalenfragmente Bioturbation, schwarze Flecken, grüne Flecken
LSL2	277	300	Tt	2,5Y 6/2	Di	S, F	F	0	c3	h1	wenige/keine auffallende Flecken
LSL1	300	350	Tt	5Y 5/1		SV, F	F	0	c2	h1	Andere sehr helle Flecken
LSL2	350	399	Tt	5Y 4/1		SV, MG	F	0	c2	h1	Schöne grüne Flecken (GLEY 1 7/56) Hellere graue Flecken 359-389: Schalenreste
LSL1	402	454	Tt	5Y 6/2 5Y 5/1		SV, F	F	0	c2	h2	402-408: Gelbe Flecken 413-453: Grüne Flecken GLEY 1 4/106Y 433-438: Wenige Schalenfragmente
LSL1	500	518	Tt	5Y 6/6 Gelbe Flecken	A	W, F	F	0	c2	h1	Wenige Schalenfragmente
LSL1	518	578	Tt	GLEY 4/56 Grüne Flecken		W, F Ab 560 minimal sichtbare Lamina-tion	F	0	c2	h2	Grüne Flecken, nach unten mehr 558-578: Viele grüne Flecken
LSL1	700	729	Tt	GLEY 5/10Y	De	SV, G	F	0	c3	h1	Bioturbation Sehr viele Flecken, schwierig zu sehen was die originale Farbe ist
LSL1	729	798	Tt	2,5Y 4/1		W, F	F	3, gr	c2	h2	
LSL1	800	833	Tt	5Y 4/1 5Y 5/2	De	W, G	F	0	c2	h2	von dunklem Ton in helleren Ton
LSL1	833	863	Tt	5Y 4/1		K	F	3, gr	c2	h2	Ton mit gröberen Körnern vor allem 833-845
LSL1	900	971	Tt	5Y 4/1	S	S, G	F	0	c2	h2	Langweiliger Ton
LSL1	971	975	Tt	5Y 5/1	De	K	F	0	c3	h1	kleiner Interfall mit hellerem Ton
LSL1	975	1000	Tt	5Y 4/1		W, G	F	0	c3	h2	
LSL1	1000	1033	Tt	5Y 3/1	De	V, G	F	0	c2	h2	
LSL1	1033	1054	Tt	5Y 4/1	De	W, F	F	2, gr	c2	h2	Schalenfragmente Schwarze, pure Tonflecken (klein)
LSL1	1054	1083	Tt	5Y 2,5/1	S	SV, G	F	2, gr	c3	h3	Schalenfragmente Schwarze, pure Tonflecken (groß)
LSL1	1083	1100	Tt	5Y 3/1		W, F	F	3, gr	c3	h3	Viele Schalenfragmente
LSL1	1100	1162	Tt	5Y 3/1	Di	bis 1130 K dann V, G	F	2, gr	c3	h3	Viele Schalenfragmente Flecken ab 1130 sind die nächste Schicht
LSL1	1162	1170	Tt	GLEY 1 6/56Y		bis 1168 V, G dann K	F	0	c3	h1	Komischer grüner Ton, am Ende mehr beige

To achieve a better illustration of the gained data the following stratigraphy was plotted.

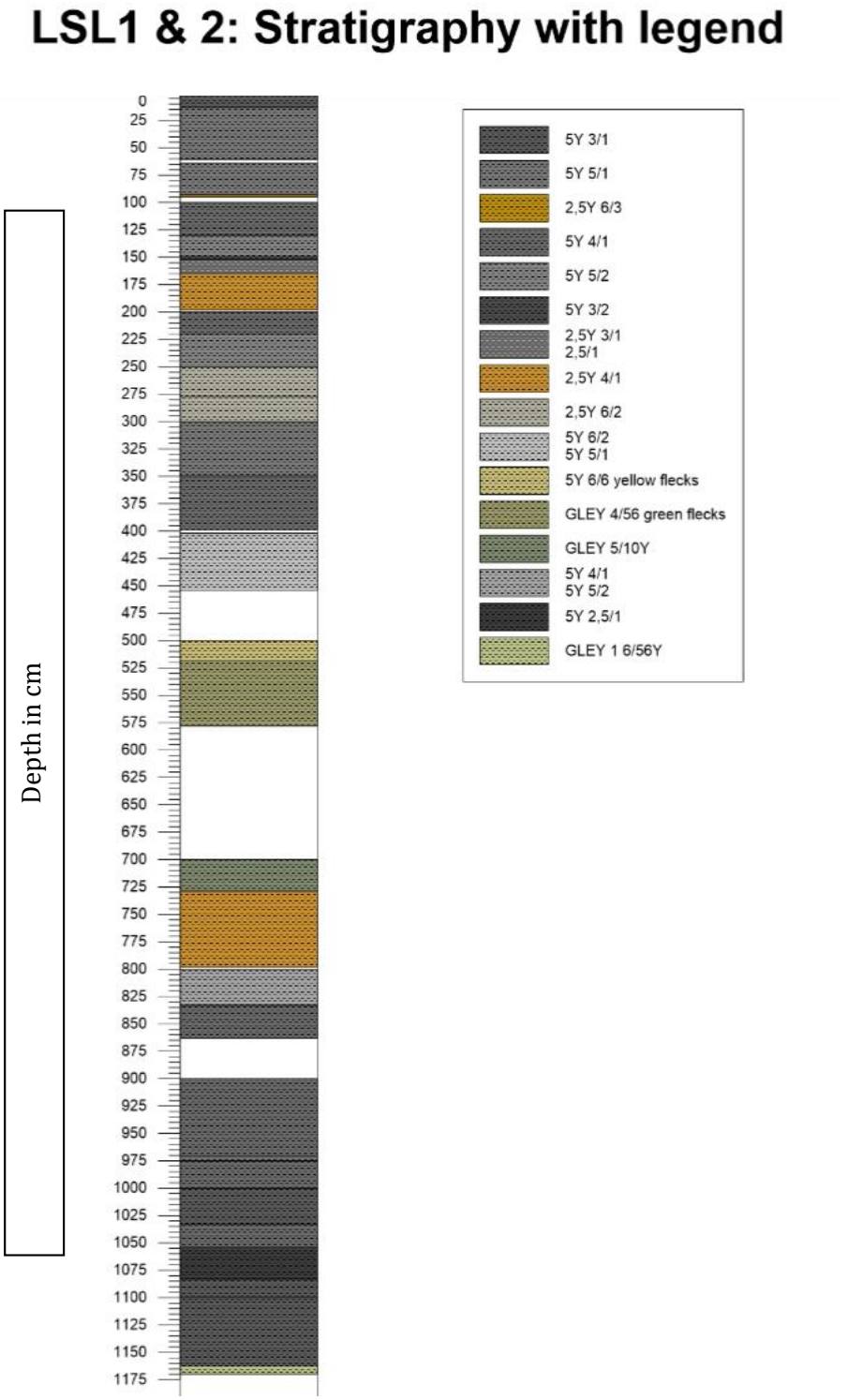

Figure 17 *- Stratigraphy of the correlated sedimentary sequence of the drilling cores LSL1 and LSL2 (Image source: Strater 4)*

The stratigraphy plot was filled by using the Munsell color system, gaps without any information were left out and are displayed in white.

The main colors represented in the sequence range between bright grey and dark grey. Only in the sequences between 165 cm and 200 cm as well as between 730 cm and 795 cm the color is clearly dark yellow to brown.

Apart from this between 500 cm and 520 cm yellow flecks are recognizable. In the subsequent range until a depth of 580 cm the color of the flecks turn into green. With the appearance of the yellow and green flecks also the entire color of the sedimentary sequence changes from yellow (range of yellow flecks) to reed green. About one meter deeper at around 700 cm the green color turns more and more into a mixture of green and grey until at 730 cm the color turns again into Peru brown. At the end of the sequence there is another color change from gunmetal/charcoal grey to a dark yellowish green (olive) at around 1,160 cm. The last information is at 1,170 cm, the sequence thus ends with this olive green.

The soil type is loamy clay in the whole sequence.

The type of the lower layer boundaries varies widely. There are only two layer boundaries which are very clear and sharp. The one at 900 cm and the one at 1,054 cm.

Along the whole sequences there are multiple layers with flecks recognizable. The amount, size and color of these flecks also vary widely. Already in the first centimeters green, yellow and white flecks do exist.

The most flecks can be found between:

- 152 cm and 250 cm
- 300 cm and 454 cm
- 700 cm and 729 cm
- 1,054 cm and 1,083 cm

The biggest flecks can be found between:

- 130 cm and 277 cm
- 700 cm and 729 cm
- 800 cm and 833 cm
- 900 cm and 971 cm
- 975 cm and 1033 cm
- 1,054 cm and 1,083 cm
- 1,130 cm and 1,168 cm

As the soil type also the moistness doesn't change during the whole sequence. All sediment layers are wet.

What is more interesting, on the other hand, is the coarse amount of the layers. While in the first 729 cm there is only one short sequence between 250 cm and 277 cm where a small percentage of coarse matter exists, however, as of 729 cm until the end the coarse amount is clearly increased up to 10 – 30 %.

The Carbonate contents are as consistent as the soil type and the moistness. They vary between a small percentage (0.5 % – 2 %) and a moderate percentage (2 % - 10 %).

A similar result can also be found concerning the organic matter. During the whole sequence there is always at least a small percentage of organic matter contained. This percentage ranges until up to 4 % (149 cm to 165 cm and 1,054 cm to 1,162 cm).

Apart of this there are a few specific mentionable observations we made while analyzing the core as for example the gypsum contents. More or less through the whole sequence there is gypsum contained, either as white flecks, as little pieces of gypsum or even as crystals. Another specialty were all the shell fragments which can also be found in the whole core, mostly in the first meter, especially as of 200 cm until a depth of 277 cm, from 402 cm to 518 cm and almost at the end from 1,033 cm to 1,162 cm.

In addition, bioturbation was found in a few sequences (152 cm to 165 cm, 250 cm to 277 cm and 700 cm to 729 cm).

The last outstanding observation we made was a thin interval of bright clay in the middle of dark grey, almost black clay at a depth of 971 cm to 975 cm.

CNS ANALYSIS

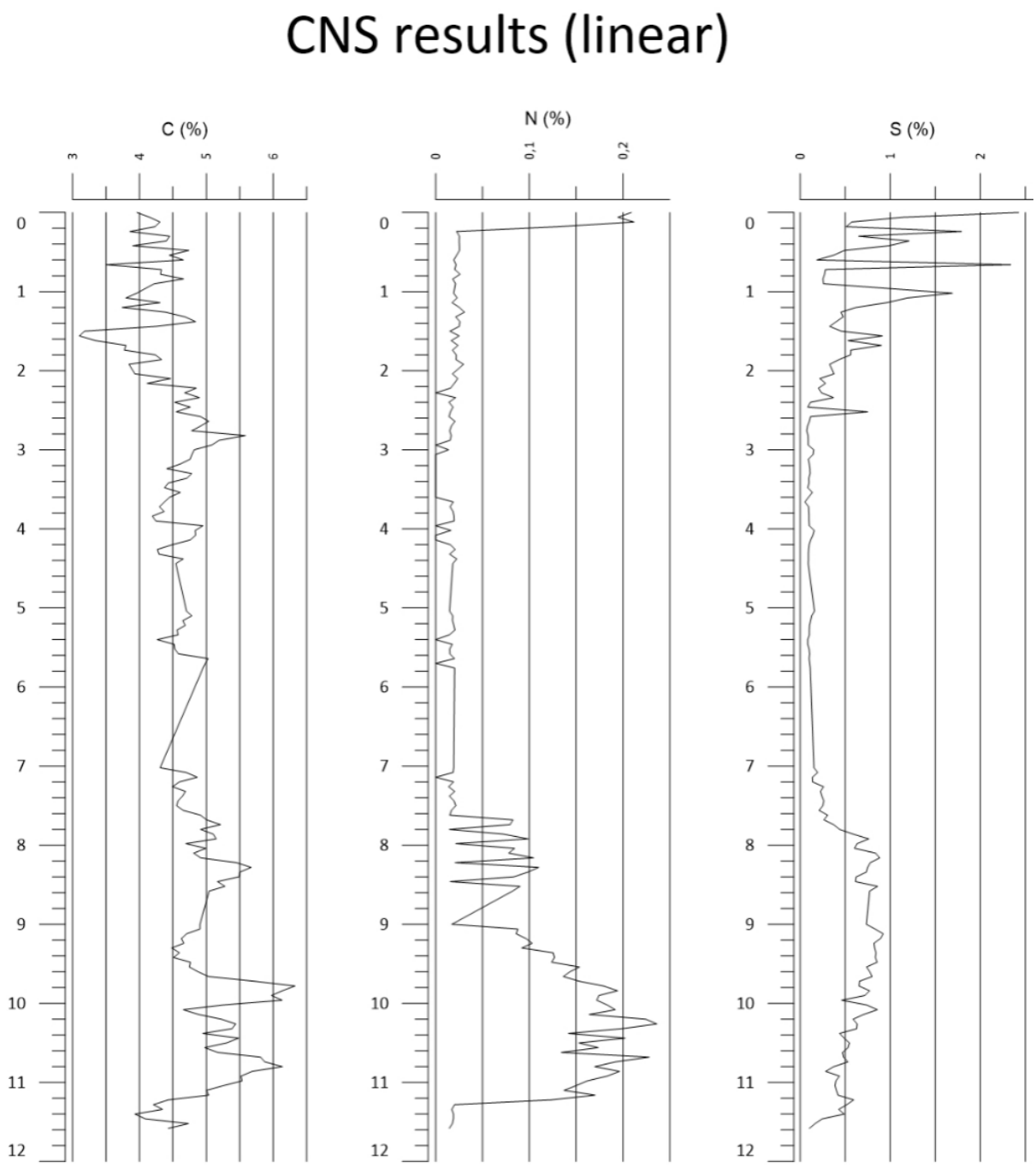

Figure 18 *- Plotted results of the CNS Analysis. The analyzed core reaches a depth of 11.7 m and C, N and S are plotted with their weight percentage.*
(Image source: Strater 4)

The displayed plot above illustrates the results of the CNS Analysis. The values for Carbon, Nitrogen and Sulfur were plotted and since the values don't range that widely the chosen axis type is linear. As already mentioned in (**6.1**) the whole sequence contains gaps without any information. These sections were surveyed carefully in the plot and since they didn't lead to any misunderstandings the data were plotted continuously. Since there were no information

available yet for TIC[13] and TOC[14] values the C/N ratio couldn't be plotted. Thus the value of Carbon represents the TC[15] value. The same holds true Nitrogen and Sulfur, the correct term of the displayed values is Total Nitrogen (TN) and Total Sulfur (TS).

The weight percentage of Carbon ranges between 3 % at a depth of around 1.5 m and almost 6.5 % at a depth of around 9.8 m and 10.8 m. The general trend is increasing downwards. Except one peak at about 2.9 m depth (5.5 %) the Carbon content stays below 5 % in the first around 7.5 m. For the rest of the core the value is predominantly over 5 % with one clear peak at around 11.4 m depth and a value of slightly less than 4 %.

The highest peak is at a depth of 9.78 m to 9.8 m with 6.33 % while the lowest peak is at a depth of 1.56 m to 1.58 m with 3.10 % (**Table 2**).

The weight percentage of Nitrogen ranges between 0 % and about 0.25 % at a depth of around 10.3 m. There is no such a trend recognizable as in the Carbon plot. Nevertheless, the plot reveals some distinctive sections of Nitrogen accumulations. During the first 7.6 m the amount of Nitrogen in the core is really low and never exceeds 0.03 %, sometimes the value is even 0. Only in the first 20 cm there are Nitrogen values around 0.2 %. Between 7.6 m and 9 m there is a sequence in which the value for Nitrogen goes up to 0.11 %. Afterwards, the Nitrogen percentage increases continuously again until it reaches its highest peaks with around 0.2 % - 0.25 % in depths between 10.2 m and 10.7 m.

The highest peak is at a depth of 10.26 m to 10.28 m with 0.24 % (**Table 2**) while the sections without any Nitrogen can be found between 2.2 m and 7.2 m.

The weight percentage of Sulfur ranges between values below 0.1 % and 2.5 % close to the surface. The plot has roughly three striking sections. The first one ranges between the surface and a depth of 2.6 m with several high peaks and a decreasing trend downwards. The second one forms the middle of the core as of a depth of 2.6 m until 7.6 m. It characterized by continuously low values without any peaks. The third section forms the lower end of the core beginning at a depth of 7.6 m and ending at 11.7 m. The Sulfur increases again in this section

[13] TIC is an abbreviation for the term Total Inorganic Carbonate
[14] TOC is an abbreviation for the term Total Organic Carbonate
[15] TC is an abbreviation for the term Total Carbonate

without exceeding 1 %. The values are quite stable in this last section, however, they decrease again after about 10.2 m.

The highest peak is besides the surface value of 2.43 % the value in a depth of 0.66 m to 0.68 m with 2.34 % Sulfur. The lowest value can be found in a depth of 3.66 m to 3.68 m with 0.05 % (**Table 2**).

X-RAY FLUORESCENCE (XRF)

The following plots illustrate the results of the XRF Analysis. From more than 35 elements detected by the XRF Scanner nine elements as well as eight elemental ratios were chosen, which allow to draw conclusions about the climatic and cultural past of the study area. As already in the CNS – Analysis and the modelling of the stratigraphy the analysis refers to the drilling core LSL1&2 with a length of 11.7 m and contains gaps without any information, which were fixed as good as possible. However, the fact that especially the samples right before and after these gaps are eventually defective should be kept in mind while analyzing the plots.

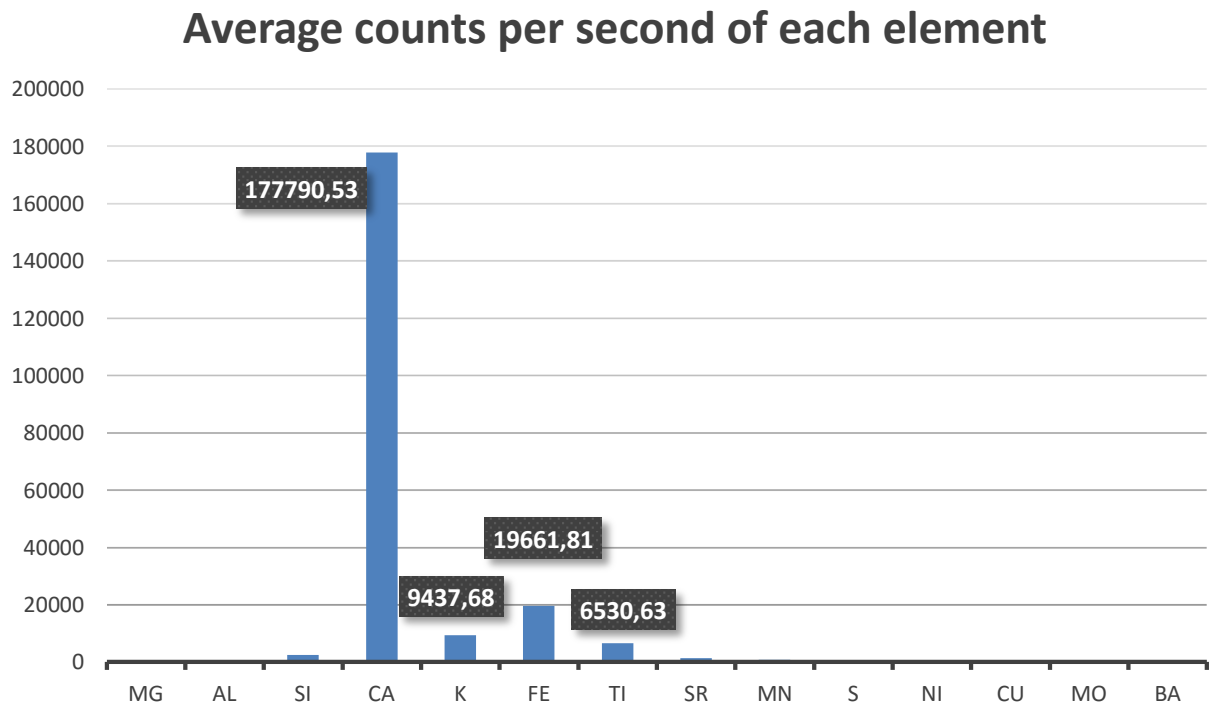

Figure 19 *- Bar chart of the average counts per second of each element used in this thesis detected by the XRF-Analysis*

The bar chart (**Figure 19**) gives a brief overview above the magnitudes of the elements. While Calcium is by far the most abundant element, followed by Iron, Potassium and Titanium are the other elements with cps below 3,000 much less abundant.

Silicon, Titanium, Sulfur

The amount of Silicon (**Figure 20**) mainly ranges between 1,000 and 3,500 cps (counts per second). During the first meter the value is increasing until 3,500. Between 1 m and 1.6 m the value increases again from 1,000 to 3,500. Afterwards the value is more or less stable at around 2,750 cps. Between 4.25 m and 4.5 m the value decreases to 2,000 cps and increases slightly at the end of the sequence. Between 5 m and 5.7m the value is stable again at around 3,000 to 3,500 cps. From 7 m to 8.6 m the value ranges slightly above 2,000 cps with a peak at around 7.75 m and a value of 3,250 cps. From 9 m until 11.5 m the value increases continuously from 1,500 to 3,250 cps. From this peak until the end of the core Silicon decreases a bit to a value of about 2,100 cps.

The plot of Titanium is very similar to the Si-plot with only a few exceptions. The peak at 5 m and 5.25 m is clearly higher. Also the curve has a distinctive peak at a depth of around 10.75 m. Overall the value for Titanium ranges between 2,500 cps at the beginning and 11,000 cps.

Sulfur has a completely different distribution in the sequence. While in the first 2 m several peaks appear with values of up to 15,000 cps, the amount of Sulfur afterwards is very small and only exceeds 2,400 cps at around 11 m.

Aluminium, Potassium, Iron

The plots of Aluminium and Potassium (**Figure 21**) show a similar behavior like the plots of Silicon and Titanium. The peak at 1.6 m is less clear and the number of cps of Aluminium is way smaller though and ranges between 70 cps and 350 cps.

The average value of Potassium is much bigger and ranges between 3,500 cps and 13,500 cps.

Iron shows so a similar plot whereas the first meter is different. The value is less increasing but already starts with a higher value and is then relatively stable. Another difference is one peak in the first meter up to more than 36,000 cps. In general, the value for Iron ranges between 8,500 cps and 38,500 cps.

CALCIUM, STRONTIUM, COPPER

The plots of Calcium and Strontium (**Figure 22**) are very similar to each other but distingiush obviously from the plots of Si, Ti, Al, K and Fe.

Calcium ranges between 40,000 cps and 280,000 cps and thus is the most represented element in the sequence. During the first meter Calcium increases from around 40,000 cps up to 250,000 cps. After the gap at around 1 m it starts again at around 70,000 cps and increases until almost 220,000 cps at a depth of around 1.4 m. Subsequently follows a decrease down to less than 10,000 cps at around 1.6 m. Except one negative peak at slightly under 2 m the value now increases again up to peaks of 280,000 cps at 2.3 m and 2.8 m. Between these peaks the value ranges around 220,000 cps. After the second peak the graph is constantly decreasing with one little peak at around 4.1 m (245,000 cps) down to a value of about 180,000 cps. The sequence between 5 m and 5.8 m has another peak of almost 270,000 cps. Between 7 m and 8.65 m the value is more of less stable. From 9 m until the end Calcium is first stable at slightly over 12,000 cps and after an increase at 9.7 m again relatively stable and varies around 16,000 cps. During the last 15 cm another increase is recognizable up to almost 290,000 cps.

The plot of Strontium is very similar to Calcium. It just ranges between smaller numbers of 600 to 2,400 cps.

Copper has another completely different appearance and no clear peaks, neither in negative nor in positive direction. The value is often 0 while occasionally values of around 150 are reached.

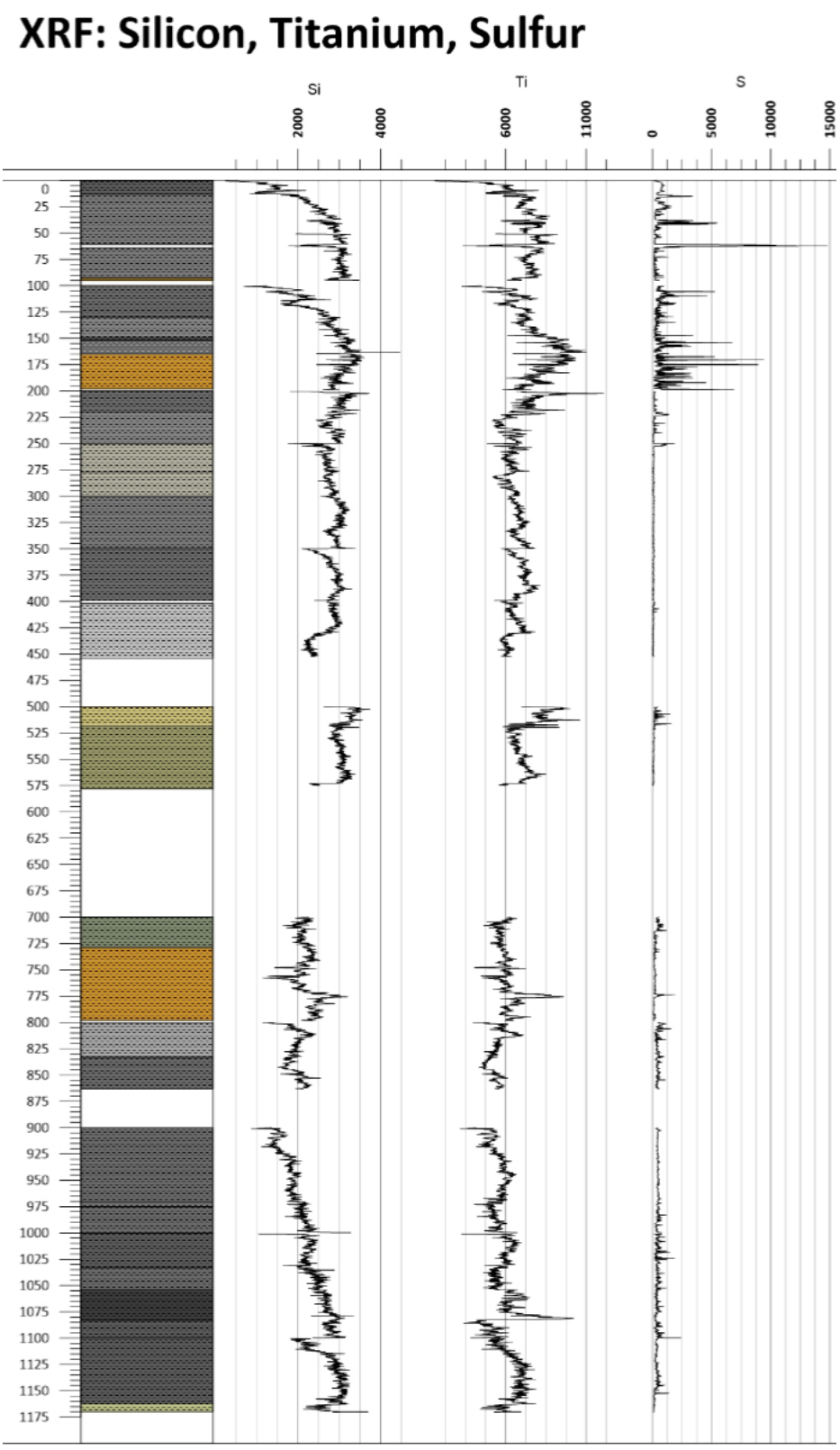

Figure 20 *- Results of the XRF-Analysis plotted next to the stratigraphy.*
Plotted elements: Silicon, Titanium, Sulfur
(Image source: Strater 4)

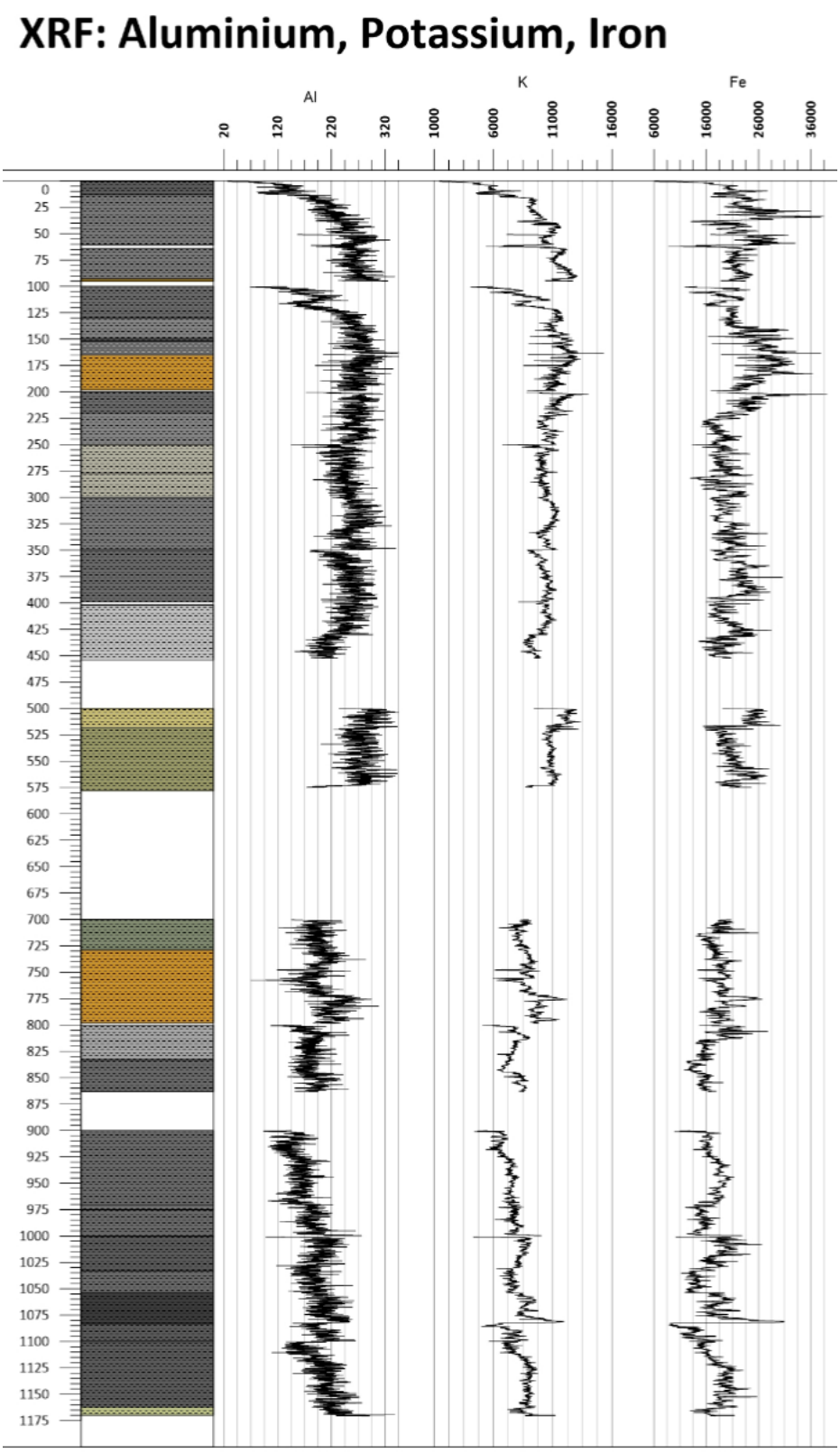

Figure 21 *- Results of the XRF-Analysis plotted next to the stratigraphy.*
Plotted elements: Aluminium, Potassium, Iron
(Image source: Strater 4)

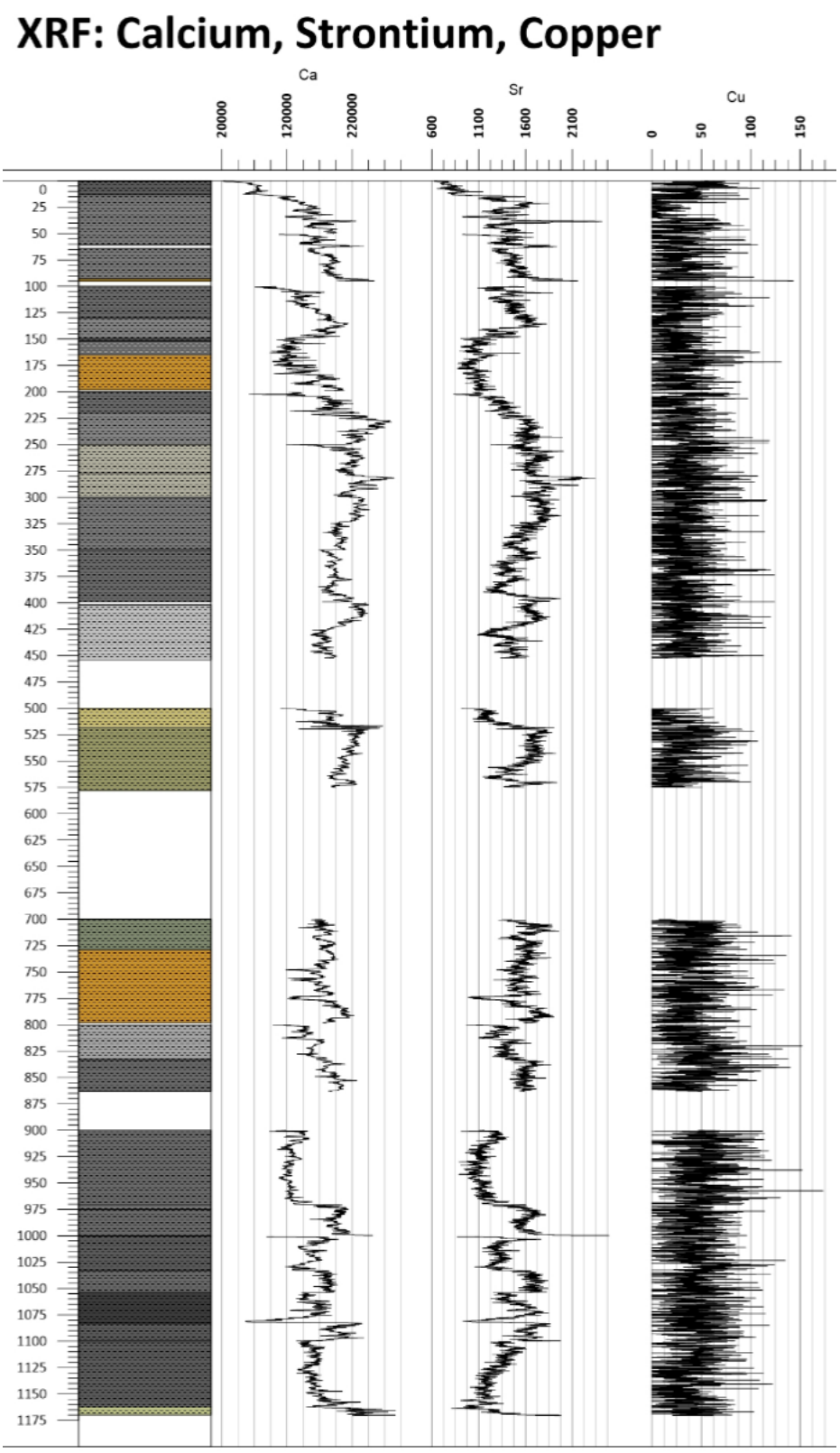

Figure 22 *- Results of the XRF-Analysis plotted next to the stratigraphy.*
Plotted elements: Calcium, Strontium, Copper
(Image source: Strater 4)

RATIOS I

The first plotted ratio is Ca/Al (**Figure 23**). Similarities to the Calcium and Strontium plots are identifiable. The ratio ranges between 200 and 1,325. During the first 1.5 m the ratio is quite stable at around 700 with three peaks rising up to around 1,000. Afterwards, the number of cps sinks down by 400 to 300 at around 1.6 m but recovers soon and reaches even 1,200 at a depth of 2.3 m. Thereupon the trend goes down a bit until the plot reaches 700 at a depth of around 4.5 m. The sequence from 5 m to 5.8 m is characterized by two small growth each from 400 and 500 to around 1,000. Between 7 m and 8.6 m the plot remains stable with one short peak at around 7.6 m up to over 1,700 and a following peak down to 400. In the last sequence of the core the plot fluctuates a lot. Peaks are at around 9.9 m, 10.3 m and 10.85 m as well at the end of the plot at 11.7 m. All peaks go up to at least 1,350. There is also one negative peak at 10.8 m down to almost 200.

The plot of Mg/Ca looks completely different. Due to the big numbers of Calcium, the numbers are really small and range between 0 and 0.0004. Nevertheless a few peaks are noticeable. During the first centimeters as well as around 1.7 m and 9.5 m, the average value is higher than the rest of the plot with peaks reaching 0.0003.

The third plot of the Fe/Mn ratio is again different to the others. The ratio is very stable for the whole 11.7 m. It mainly ranges between 8 and 50. While the average value for the first 5.8 m is at about 28, the sequence from 7 m until the end has first a smaller average (20) but the ratio increases over the last 1.7 m up to 38.

RATIOS II

The Mo/Al ratio (**Figure 24**) mainly ranges between 0 and 1. Occasionally peaks are indentifiable at a depth of 1 m and directly at the beginning under the surface. Furthermore, the values of the sequence between 7 m and 8.65 m and especially between 9 m and the end seem to reach higher values than the ratios in the first half of the core.

The plot for the Sr/Al ratios looks very similar to the Ca/Al plot. The numbers are much smaller though. They mainly range between 2 and 12 with peaks at the beginning, 1 m and around 7.6 m up to about 20.

The plot for Cu/Al shows as the Mo/Al ratio only slight fluctuations and mainly ranges between 0 and 1. Only a few small peaks are recognizable at the beginning and in depths of 1 m to 1.2 m, at around 8.3 m and directly after the 9 m mark.

RATIOS III

The last two ratios (**Figure 25**) are Ni/Al and Ba/Al. The plot of Ni/Al resembles the Mo/Al ratio a lot. Also the number of the ratio ranges in more or less the same intervall – between 0 and 1. However, the value 0 is rarer in this plot.

The Ba/Al ratio shows another slightly different graph. Ratios range between 0 and 4. The first 1.7 m are identical to the Ni/Al plot though. Whereas the subsequent section constantly decreases until a depth of 2.7 m and values around 0^{+}. Right afterwards the ratios are stable at around 1. Only in the last section of the core the graph shows another clear decrease until the end of the core and values between 0 and 1 after it first increased a bit from 10 m to 10.6 m and a values around 3. In this last section are also four peaks visible which exceed a value of 3, namely in depth of 9.6 m, 10.5 m, 11 m and 11.6 m.

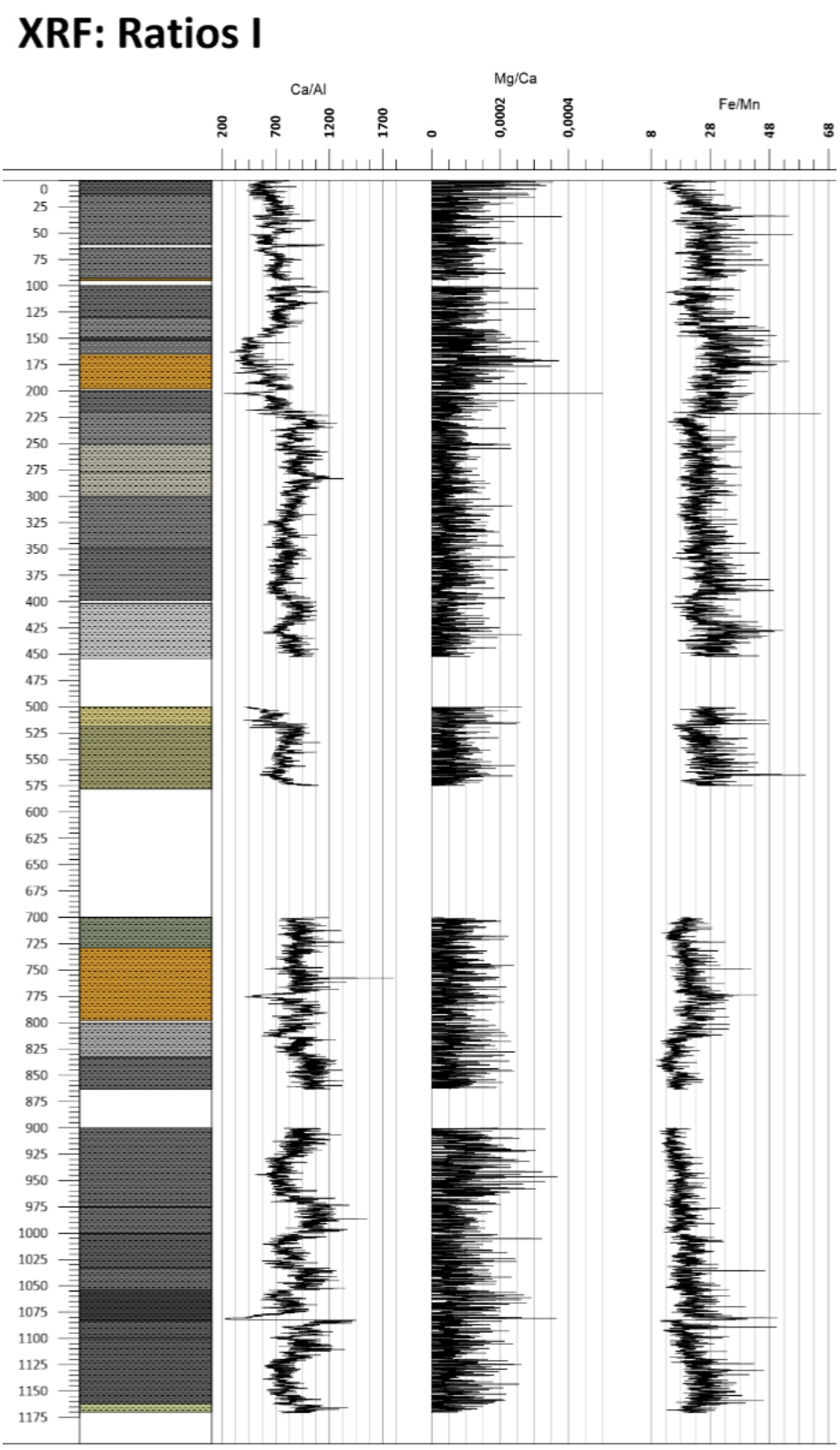

Figure 23 *- Results of the XRF-Analysis plotted next to the stratigraphy. Plotted elemental ratios: Ca/Al, Mg/Ca, Fe/Mn (Image source: Strater 4)*

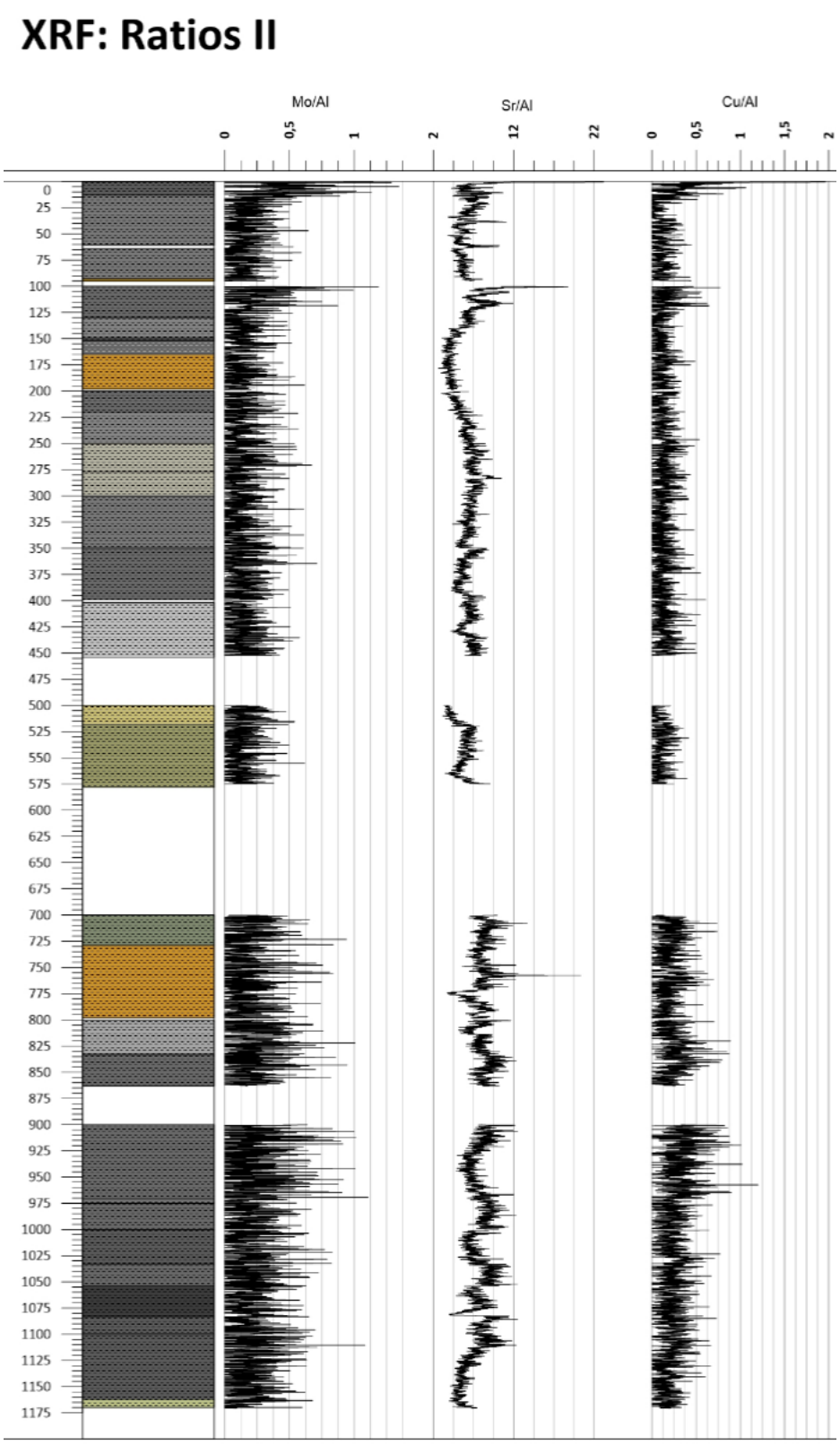

Figure 24 *- Results of the XRF-Analysis plotted next to the stratigraphy.*
Plotted elemental ratios: Mo/Al, Sr/Al, Cu/Al
(Image source: Strater 4)

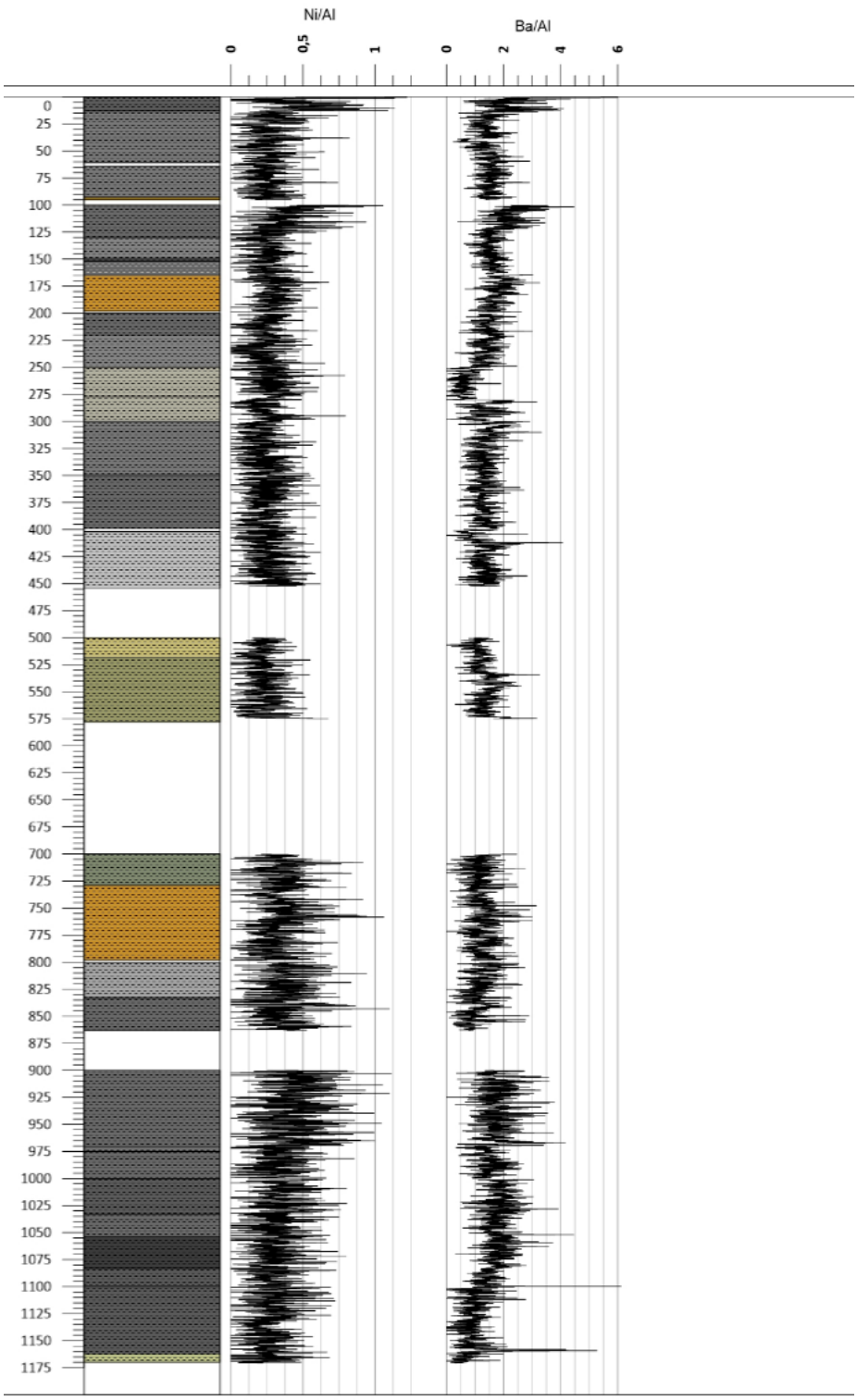

Figure 25 *- Results of the XRF-Analysis plotted next to the stratigraphy.*
Plotted elemental ratios: Ni/Al, Ba/Al
(Image source: Strater 4)

DISCUSSION AND INTERPRETATION

CNS ANALYSIS

Of all fractions of lake sediments, organic matter constitutes a minor but very important one for paleolimnological investigations. It contains organic matter in form of lipids, carbohydrates, proteins and other organic matter components produced by organisms that have lived in and around the lake. Organic matter can be seen as an accumulation of geochemical fossils and therefore provides information for interpretations of both natural and human-induced changes in the regional ecosystems which are directly related to the prevalent climate (Last & Smol, 2001b). In general, plants as source of organic matter can be divided into two geochemically distinctive groups. Non-vascular plants (phytoplankton) which contain little or no carbon-rich cellulose and lignin and vascular plants (grasses, trees) which contain large proportions of these fibrous tissues (Last & Smol, 2001b).

Since the results of our CNS Analysis show Carbon proportions which were constantly higher than 3 %, in bigger depths even with percentages exceeding 6 % the ecosystem surrounding and including the Laguna Grande was always habitat of vascular plants. Negative peaks can be an indicator for less plant growth, maybe induced by corresponding climate conditions like cold periods or ice ages. On the other hand, positive peaks like in depths of 9.8 m or 10.9 m could be an indicator for tropical conditions inducing a large amount and diversity of plants. For further investigations to determine the types and amounts of original materials as well as the extent of alteration and degradation of the starting material more extensive analyses are necessary such as the determination of TOC and TIC proportions and the associated calculation of the C/N ratio. Another factor which should be taken into account while analyzing organic matter proportions is microbial activity. During sinking and sedimentation microbial reworking diminishes the amount of organic matter while replacing many of the primary compounds with secondary ones (Last & Smol, 2001b).

Although Nitrogen is a small constituent of all organisms it is an essential nutrient and commonly viewed as one of the ultimately limiting factors of organic productivity. Thus changes in Nitrogen concentrations are directly related to significant impacts on the production, composition and accumulation of sedimentary organic matter. Thus, knowledge of past proportions of Nitrogen can enable to draw conclusions concerning local, regional or

even global environmental changes. Nitrogen is mainly characterized by its total proportion (total nitrogen (TN)) or by its ratio with Carbon (C/N ratio). Caused by the lack of information concerning TIC and TOC data, this thesis focuses on the interpretation of the TN data. It's also important to consider present additional sources of Nitrogen while analyzing especially sub surface sediments. Anthropogenic influences such as the combustion of fossil fuels and many industrial processes which discharge gaseous and particulate nitrogen compounds into the atmosphere or agriculture and urban development which led to emissions of dissolved and solid Nitrogen to surface and groundwater networks affect the concentration of Nitrogen in the lakes and hence in the sediments. The main source of Nitrogen in lake sediments has its origin in phytoplankton due to their high protein and lipid content. Terrestrial plants, on the other hand, are rather N-poor since their organic matter is dominated by cellulose and lignin. Again, the activity of microorganisms plays a decisive role. Nitrogen-fixing in soils can lead to Nitrogen enrichments, particularly around plant roots. The results of the CNS analysis show large peaks in their Nitrogen proportions in little depths and high depths. The Nitrogen peak in subsurface layers can be caused by mentioned anthropogenic effects, whereas the peaks at around 8 m and from 9 m to 11.2 m can be caused by increased microbial activity and thus higher productivity in the lake area. This interpretation would approve the assumptions made concerning the Carbon proportions in these depths (Last & Smol, 2001b).

Enrichment of Sulfur in sediments is principally related to bacterial sulfate reduction. Low oxygen availability leads to an anoxic state and organic matter remains preserved. High TS content can be traced back to sulfate reduction in anaerobic sediments; in amictic lakes this leads to hydrogen sulfide generation in bottom waters which is transformed to insoluble FeS or FeS_2 and deposited on the lake bottom. An anoxic state is also indicated by the absence of bioturbation which allows sediments to be deposited as laminations. The increased amount of TS in the first 2.5 m, especially within the first 1.2 m, as well as between 8 m to 11.5 m leads to the assumption that anoxic conditions were present during these periods. This can be approved by dark colored sediments in these depths (**Figure 17**) and the lack of bioturbation (**Table 1**). Another reason for increased Sulfur contents can be ascribed to the large amount of gypsum ($CaSO_4 \cdot 2H_2O$) prospected in the Laguna Grande. Dry periods inducing increased evaporation lead to precipitation of gypsum and thus higher Sulfur values (Eugster, 1980).

XRF ANALYSIS

Providing large amounts of data the XRF Analysis has become a valuable tool in the paleolimnology. This study focuses on the analysis and interpretation of specific elements and ratios which are elucidated in their functions as proxies in the following.

Inducing the abundance of aragonite Sr-rich sediments characterize brackish lakes (with high salinity, higher Sr/Al) while S-rich sediments indicate saline lakes with large amounts of gypsum. Both elements are proxies for lower lake levels. Sulfur is, in addition, also proxy for high salinity, whereas Strontium enrichments indicate ephemeral lake conditions.

Higher lake levels, on the other hand, are characterized by elements such as Ti and Si (which are also proxy for increased littoral erosion (allochthonous[16] compounds) and detrital input), Al, K, Fe and Mo/Al ratios.

Calcium is rather a proxy for drier periods and lake level fluctuations.

As well as the elements also the ratios are proxies for certain climate conditions. One of the most important ratios is Ca/Al. It characterizes high water mineralization, chemical weathering and the presence of gypsum. With Sr/Al and Ba/Al it also describes endogenic calcite precipitation and carbonate formation. Other chemical ratios identify evaporite precipitation (higher Sr/Al), anoxic conditions (higher Mo/Al) and higher biological activity (higher Mg/Ca, Fe/Mn). Furthermore, Mg/Ca is also a proxy for higher carbon contents and precipitation as well as Fe/Mn is also a proxy for piritization.

Cu/Al and Ni/Al characterize human impacts in terms of the usage of fertilizer or similar effects on the environment (Valero-Garcés et al., 2011).

Thus the increase of Si and Ti within the bottom sequence of the core approves the conclusion drawn from the increased organic matter found in the same section. During the period, where the sediments from the core bottom are from, the results thus describe a Laguna Grande with increased lake level (low Sr, S; high Si, Ti, Fe; overaverage Al, K, Mo/Al), low salinity (low S, Sr/Al), higher biological productivity (increased OM, high Fe/Mn), possible piritization (high

[16] The term *allochthonous* describes rocks, minerals, etc. which are not formed in the region they were found. *Autochthonous*, on the other hand, describes the opposite (formed where it was found).

Fe/Mn) and bottom anoxia (overaverage Mo/Al, increased Sulfur (CNS), dark colored sediments).

Another interesting section is between 1.4 m and 2 m. Here we have similar conditions to the bottom section described above. Especially the increased Sulfur is conspicuous. Additionally, the Mg/Ca is clearly increased at this point while Sr/Al has its lowest ratios in this section. The conditions thus seem to be very similar to those at the end of the core.

An opposite scenario could have taken place right after the section between 1.4 m and 2 m. Since the core has a gap right before 1 m depth, the data right afterwards can contain mistakes. A few centimeters lower at around 1.15 m, on the other hand, the data should be valid. The positive peaks of Sr/Al, Sr, Ca and S and the negative peaks of Si, Ti, K, Al, Fe, and Fe/Mn approve this assumption. However, since the graphs of almost all plots tent to fluctuate strongly, this interpretation needs to be proven by further investigations. In general terms, the different graphs show strong fluctuations in various sections such as between 3.7 m and 4.5 m, 7.3 m and 8.6 m and in the whole sequence before the bottom sequence which supports the statements of rapid climate changes during the Holocene (Collaborative Research Center 806, 2009; Nieto-Moreno et al., 2011).

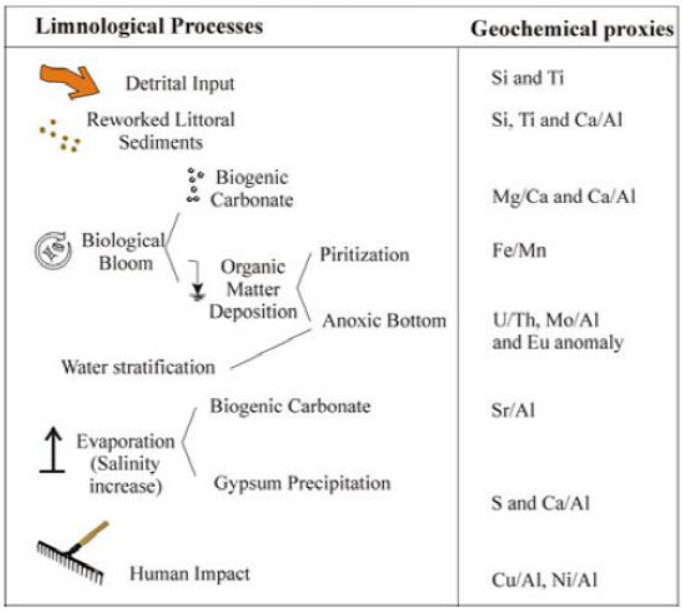

Figure 26 *- Limnological processes and their relation to geochemical proxies (Image source: Martin Puertas, C.,Valero-Garcés, B. L., Pilar Mata, M., Moreno, A., Giralt, S., Martínez-Ruiz, F., Jiménez-Espejo, F., 2009. Geochemical processes in a Mediterranean Lake: a high-resolution study of the last 4,000 years in Zoñar Lake, southern Spain)*

CONCLUSION

High-resolution geochemical data obtained by CNS and XRF analysis in conjunction with a macroscopic description of the correlated drilling core LSL1&2 conducted in the Laguna Grande provide information which help to reconstruct the paleoclimate of the Holocene of the southern Iberian Peninsula.

By interpreting the available results the constructed hypotheses read as follows. Ascribed to peaks and variations in specific plots of elemental proportions, elemental ratios and organic matter components, the sequence drilled in the lake shows high climate fluctuations representing the typical rapid climate changes of the Holocene as well as cold periods or ice ages and rather dry periods with high salinity. Since the plots of copper or nickel barely reveal any clear anomalies it's hard to say if there was a big anthropogenic influence.

Although contextualizing of several data leads to a rough estimation of climatic conditions, further investigations are necessary to complete and validate constructed hypotheses. These investigations could be isotope dating to obtain information concerning the point of time of the described climatic reconstructions. Also an analysis of the Total Carbon would be helpful since C/N ratios represent a powerful tool of paleoclimatology. Another improvement could be the completing of the drilling core. The lack of information concerning the sections without any samples prevents a continuous reconstruction. Furthermore, several sections, especially right after and before the gaps, seem to display inaccurate data which can lead to misinterpretations and incorrect conclusions.

OUTLOOK

The spreading of the Homo sapiens during the Holocene represents a research area we all can identify with and we all should be interested in since it's actually the story of our all ancestors (in geological scales). Moreover, the fact that we do have the possibilities as scientists from highly developed countries to conduct fundamental research we should have an obligation in reconstructing the pathways of our own unique species. The Collaborative Research Center 806 contributes to this idea and aims to provide new knowledge in this area. Thus the aspiration of the project C3 should be a complete as possible reconstruction of the paleoclimate of the Iberian Peninsula while finding ourselves in an intellectual exchange with scientists of all affected areas and countries.

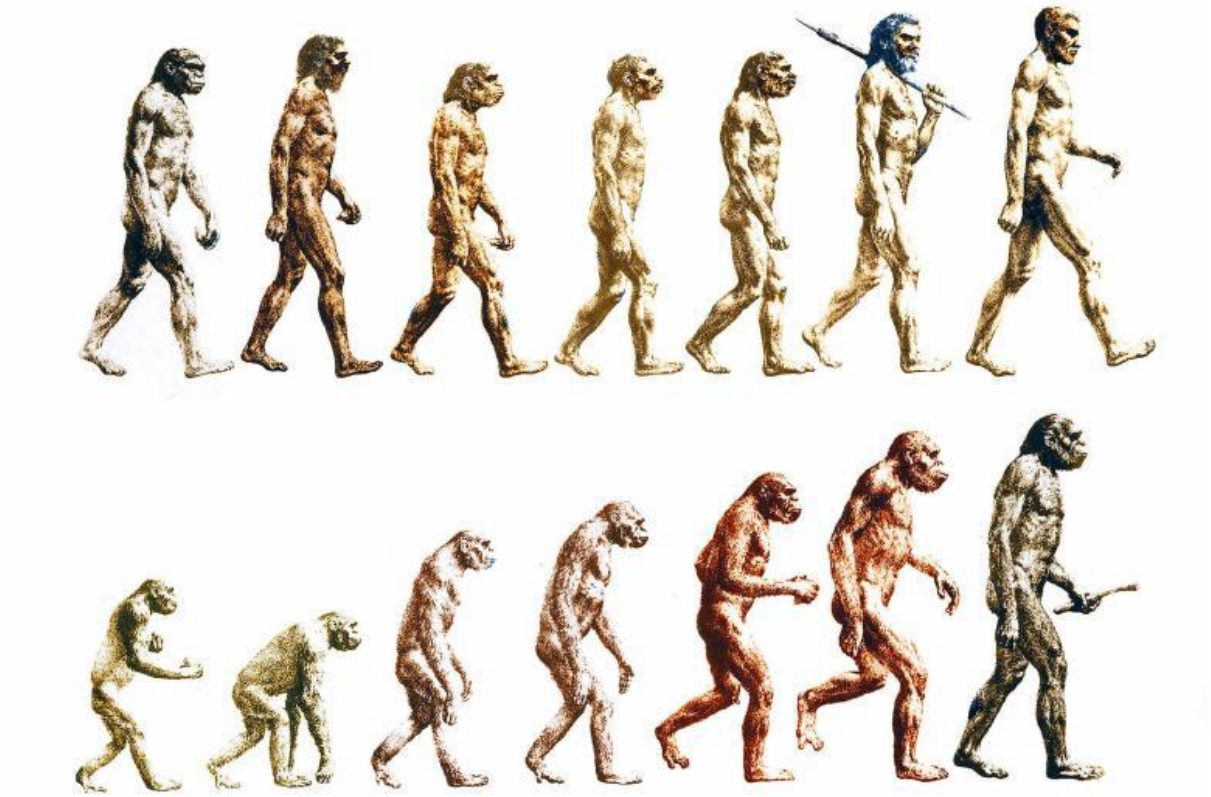

Figure 27 *- From ape-like creatures (bottom left) to the Homo sapiens (top right)*
(Image source: Frankenfeld, T., 2013. Hat der Mensch seine eigene Evolution gestoppt?, newspaper article digitally published on September 12, 2013 on welt.de
URL: http://www.welt.de/wissenschaft/article119945856/Hat-der-Mensch-seine-eigene-Evolution-gestoppt.html)

REFERENCES

Battarbee, R. (2000). Palaeolimnological approaches to climate change, with special regard to the bioogical record. *Quaternary Science Reviews*, *19*, 107–124.

Cacho, I., Grimalt, J. O., Pelejero, C., Canals, M., Sierro, F. J., Flores, J. A., & Shackleton, N. (1999). Dansgaard-Oeschger and Heinrich event imprints in Alboran Sea paleotemperatures. *Paleoceanography*, *14*(6), 698–705. http://doi.org/10.1029/1999PA900044

Central Intelligence Agency. (2014). The World Factbook. Retrieved from https://www.cia.gov/library/publications/the-world-factbook/geos/sp.html

Collaborative Research Center 806. (2009). Our Way To Europe - Introduction.

Comin, F. a., & Alonso, M. (1988). Spanish salt lakes: Their chemistry and biota. *Hydrobiologia*, *158*(1), 237–245. http://doi.org/10.1007/BF00026281

Croudace, I. W. (2006). ITRAX : Description and evaluation of a new multi-function X-ray core scanner, (September 2015). http://doi.org/10.1144/GSL.SP.2006.267.01.04

Elementar Analysensysteme GmbH. (n.d.). *vario MICRO tube*.

Eugster, H. P. (1980). Geochemistry of Evaporitic Lacustrine Deposits. *Annual Review of Earth and Planetary Sciences*, *8*(1), 35–63. http://doi.org/10.1146/annurev.ea.08.050180.000343

Gibbons, W., & Moreno, T. (2002). *The Geology of Spain*. The Geological Society London.

González-Castillo, L., Galindo-Zaldívar, J., Junge, A., Martínez-Moreno, F. J., & Löwer, A. (2015). Tectonophysics Evidence of a large deep conductive body within the basement of the Guadalquivir foreland Basin (Betic Cordillera , S-Spain) from tipper vector modelling : Tectonic implications a. *Tectonophysics*. http://doi.org/10.1016/j.tecto.2015.08.013

Iacobellis, V., Castorani, A., Rosario, A., Santo, D., & Gioia, A. (2015). Rationale for flood prediction in karst endorheic areas. *Journal of Arid Environments*, *112*, 98–108. http://doi.org/10.1016/j.jaridenv.2014.05.018

Junta de Andalucia. (2003). Lagunas Salada , Chica y Juncosa, (Primavera), 113–122.

Last, W. M., & Smol, J. P. (2001a). *Tracking Environmental Change Using Lake Sediments, Volume 1: Basin Analysis, Coring and Chronological Techniques* (Vol. 1).

Last, W. M., & Smol, J. P. (2001b). *Tracking Environmental Change Using Lake Sediments. Volume 2: Physical and Geochemical Methods* (Vol. 2).

Martín-Puertas, C. (2010). Late Holocene climate variability in the southwestern Mediterranean region : an integrated marine and terrestrial geochemical approach, 807–816. http://doi.org/10.5194/cp-6-807-2010

Nieto-Moreno, V., Martínez-Ruiz, F., Giralt, S., Jiménez-Espejo, F., Gallego-Torres, D., Rodrigo-Gámiz, M., De Lange, G. J. (2011). Tracking climate variability in the western Mediterranean during the Late Holocene: A multiproxy approach. *Climate of the Past*, *7*(4), 1395–1414. http://doi.org/10.5194/cp-7-1395-2011

Podbregar, N., Schwanke, K., & Frater, H. (2009). *Wetter , Klima , Klimawandel*.

Reicherter, K. R., & Peters, G. (2005). Neotectonic evolution of the Central Betic Cordilleras (Southern Spain). *Tectonophysics*, *405*(1-4), 191–212. http://doi.org/10.1016/j.tecto.2005.05.022

Serrano, I., Torcal, F., & Benito, J. (2015). Tectonophysics " High resolution seismic imaging of an active fault in the eastern Guadalquivir Basin (Betic Cordillera , Southern Spain) ." *Tectonophysics*. http://doi.org/10.1016/j.tecto.2015.08.020

Valero-Garcés, B. L., Martín Puertas, C., Mata, M. P., Moreno, A., Giralt, S., Jiménez-Espejo, F., & Martínez-Ruiz, F. (2011). Geochemical processes in a Mediterranean Lake: a high-resolution study of the last 4,000 years Zoñar Lake, southern Spain, 405–421. http://doi.org/10.1007/s10933-009-9373-0

APPENDIX

Table 2 *– Results of the CNS Analysis*

Hole ID	Depth		C (%)	N (%)	S (%)
	from	**to**			
LSL 1	0	0,02	**3,96**	**0,21**	**2,427**
LSL 1	0,06	0,08	**4,15**	**0,19**	**1,145**
LSL 1	0,12	0,14	**4,31**	**0,21**	**0,572**
LSL 1	0,18	0,2	**4,23**	**0,13**	**0,512**
LSL 1	0,24	0,26	**3,86**	**0,02**	**1,792**
LSL 1	0,3	0,32	**4,45**	**0,03**	**0,650**
LSL 1	0,36	0,38	**4,40**	**0,03**	**1,210**
LSL 1	0,42	0,44	**3,90**	**0,03**	**0,987**
LSL 1	0,48	0,5	**4,74**	**0,03**	**0,491**
LSL 1	0,54	0,56	**4,45**	**0,02**	**0,371**
LSL 1	0,6	0,61	**4,65**	**0,02**	**0,186**
LSL 1	0,66	0,68	**3,50**	**0,02**	**2,338**
LSL 1	0,72	0,74	**4,33**	**0,02**	**0,282**
LSL 1	0,78	0,8	**4,31**	**0,03**	**0,272**
LSL 1	0,84	0,86	**4,66**	**0,02**	**0,253**
LSL 1	0,9	0,92	**4,22**	**0,02**	**0,259**
LSL 1	1,02	1,04	**3,96**	**0,02**	**1,691**
LSL 1	1,08	1,1	**3,80**	**0,02**	**1,191**
LSL 1	1,14	1,16	**4,31**	**0,02**	**0,962**
LSL 1	1,2	1,22	**3,74**	**0,03**	**0,621**
LSL 1	1,26	1,28	**4,39**	**0,03**	**0,454**
LSL 1	1,32	1,34	**4,68**	**0,02**	**0,478**
LSL 1	1,38	1,4	**4,84**	**0,03**	**0,400**
LSL 1	1,44	1,46	**4,25**	**0,03**	**0,328**
LSL 1	1,5	1,52	**3,18**	**0,02**	**0,456**
LSL 1	1,56	1,58	**3,10**	**0,02**	**0,913**
LSL 1	1,62	1,64	**3,34**	**0,02**	**0,531**
LSL 1	1,68	1,7	**3,80**	**0,02**	**0,902**
LSL 1	1,74	1,76	**3,78**	**0,02**	**0,562**
LSL 1	1,8	1,82	**4,24**	**0,02**	**0,561**
LSL 1	1,86	1,88	**4,33**	**0,02**	**0,431**
LSL 1	1,92	1,94	**3,84**	**0,03**	**0,327**
LSL 1	2,04	2,06	**3,93**	**0,02**	**0,377**
LSL 1	2,1	2,12	**4,47**	**0,02**	**0,218**
LSL 1	2,16	2,18	**4,11**	**0,02**	**0,282**
LSL 1	2,22	2,24	**4,85**	**0,02**	**0,204**
LSL 1	2,28	2,3	**4,68**	**0,00**	**0,236**
LSL 1	2,34	2,36	**4,90**	**0,02**	**0,371**
LSL 1	2,4	2,42	**4,53**	**0,01**	**0,114**
LSL 1	2,46	2,48	**4,76**	**0,02**	**0,084**
LSL 1	2,52	2,54	**4,55**	**0,02**	**0,751**
LSL 1	2,58	2,6	**4,91**	**0,01**	**0,116**
LSL 1	2,64	2,66	**5,04**	**0,02**	**0,102**

LSL 1	2,7	2,72	**4,91**	**0,02**	**0,082**
LSL 1	2,76	2,78	**4,78**	**0,01**	**0,073**
LSL 1	2,82	2,84	**5,58**	**0,02**	**0,088**
LSL 1	2,88	2,9	**5,19**	**0,02**	**0,090**
LSL 1	2,94	2,96	**5,08**	**0,00**	**0,090**
LSL 1	3	3,02	**4,82**	**0,01**	**0,149**
LSL 1	3,06	3,08	**4,78**	**0,00**	**0,143**
LSL 1	3,12	3,14	**4,76**	**0,00**	**0,091**
LSL 1	3,18	3,2	**4,61**	**0,00**	**0,102**
LSL 1	3,24	3,26	**4,41**	**0,00**	**0,109**
LSL 1	3,3	3,32	**4,78**	**0,00**	**0,110**
LSL 1	3,36	3,38	**4,71**	**0,00**	**0,097**
LSL 1	3,42	3,44	**4,43**	**0,00**	**0,098**
LSL 1	3,48	3,5	**4,38**	**0,00**	**0,085**
LSL 1	3,54	3,56	**4,61**	**0,00**	**0,136**
LSL 1	3,6	3,62	**4,45**	**0,00**	**0,093**
LSL 1	3,66	3,68	**4,37**	**0,02**	**0,052**
LSL 1	3,72	3,74	**4,30**	**0,02**	**0,094**
LSL 1	3,78	3,8	**4,37**	**0,02**	**0,096**
LSL 1	3,84	3,86	**4,19**	**0,02**	**0,099**
LSL 1	3,9	3,92	**4,25**	**0,02**	**0,099**
LSL 1	3,96	3,98	**4,95**	**0,00**	**0,102**
LSL 1	4,02	4,04	**4,83**	**0,02**	**0,155**
LSL 1	4,08	4,1	**4,84**	**0,00**	**0,141**
LSL 1	4,14	4,16	**4,76**	**0,00**	**0,117**
LSL 1	4,2	4,22	**4,49**	**0,02**	**0,100**
LSL 1	4,26	4,28	**4,27**	**0,02**	**0,094**
LSL 1	4,32	4,34	**4,29**	**0,01**	**0,091**
LSL 1	4,38	4,4	**4,65**	**0,02**	**0,093**
LSL 1	4,44	4,46	**4,54**	**0,02**	**0,090**
LSL 1	5,04	5,06	**4,70**	**0,01**	**0,158**
LSL 1	5,1	5,12	**4,78**	**0,02**	**0,128**
LSL 1	5,16	5,18	**4,65**	**0,02**	**0,116**
LSL 1	5,22	5,24	**4,68**	**0,02**	**0,105**
LSL 1	5,28	5,3	**4,56**	**0,02**	**0,102**
LSL 1	5,34	5,36	**4,58**	**0,01**	**0,103**
LSL 1	5,4	5,42	**4,27**	**0,00**	**0,085**
LSL 1	5,46	5,48	**4,52**	**0,02**	**0,085**
LSL 1	5,52	5,54	**4,53**	**0,01**	**0,100**
LSL 1	5,58	5,6	**4,58**	**0,02**	**0,106**
LSL 1	5,64	5,66	**5,03**	**0,02**	**0,100**
LSL 1	5,7	5,72	**4,98**	**0,00**	**0,106**
LSL 1	5,76	5,78	**4,95**	**0,02**	**0,113**
LSL 1	7,02	7,04	**4,31**	**0,02**	**0,152**
LSL 1	7,08	7,1	**4,70**	**0,02**	**0,195**
LSL 1	7,14	7,16	**4,86**	**0,00**	**0,136**
LSL 1	7,2	7,22	**4,60**	**0,02**	**0,138**
LSL 1	7,26	7,28	**4,49**	**0,01**	**0,259**
LSL 1	7,32	7,34	**4,69**	**0,02**	**0,225**

X

LSL 1	7,38	7,4	**4,64**	**0,01**	**0,241**
LSL 1	7,44	7,46	**4,58**	**0,02**	**0,263**
LSL 1	7,5	7,52	**4,56**	**0,02**	**0,251**
LSL 1	7,56	7,58	**4,65**	**0,02**	**0,210**
LSL 1	7,62	7,64	**4,91**	**0,02**	**0,305**
LSL 1	7,68	7,7	**5,00**	**0,08**	**0,265**
LSL 1	7,74	7,76	**5,21**	**0,08**	**0,371**
LSL 1	7,8	7,82	**4,92**	**0,01**	**0,438**
LSL 1	7,86	7,88	**5,10**	**0,07**	**0,587**
LSL 1	7,92	7,94	**5,15**	**0,10**	**0,762**
LSL 1	7,98	8	**4,69**	**0,02**	**0,633**
LSL 1	8,04	8,06	**4,99**	**0,08**	**0,604**
LSL 1	8,1	8,12	**4,81**	**0,08**	**0,837**
LSL 1	8,16	8,18	**4,91**	**0,10**	**0,884**
LSL 1	8,22	8,24	**5,45**	**0,02**	**0,779**
LSL 1	8,28	8,3	**5,67**	**0,11**	**0,750**
LSL 1	8,34	8,36	**5,50**	**0,10**	**0,735**
LSL 1	8,4	8,42	**5,49**	**0,08**	**0,622**
LSL 1	8,46	8,48	**5,17**	**0,02**	**0,615**
LSL 1	8,52	8,54	**5,28**	**0,09**	**0,861**
LSL 1	8,58	8,6	**5,04**	**0,08**	**0,771**
LSL 1	9	9,02	**4,90**	**0,02**	**0,735**
LSL 1	9,06	9,08	**4,90**	**0,09**	**0,832**
LSL 1	9,12	9,14	**4,71**	**0,09**	**0,921**
LSL 1	9,18	9,2	**4,63**	**0,10**	**0,892**
LSL 1	9,24	9,26	**4,66**	**0,10**	**0,819**
LSL 1	9,3	9,32	**4,48**	**0,09**	**0,826**
LSL 1	9,36	9,38	**4,60**	**0,13**	**0,842**
LSL 1	9,42	9,44	**4,51**	**0,13**	**0,834**
LSL 1	9,48	9,5	**4,76**	**0,12**	**0,855**
LSL 1	9,54	9,56	**4,75**	**0,15**	**0,737**
LSL 1	9,6	9,62	**4,87**	**0,14**	**0,772**
LSL 1	9,66	9,68	**5,03**	**0,14**	**0,800**
LSL 1	9,72	9,74	**5,72**	**0,15**	**0,658**
LSL 1	9,78	9,8	**6,33**	**0,18**	**0,653**
LSL 1	9,84	9,86	**6,14**	**0,19**	**0,770**
LSL 1	9,9	9,92	**5,98**	**0,17**	**0,718**
LSL 1	9,96	9,98	**6,13**	**0,17**	**0,460**
LSL 1	10,02	10,04	**5,25**	**0,18**	**0,739**
LSL 1	10,08	10,1	**4,66**	**0,19**	**0,857**
LSL 1	10,14	10,16	**4,88**	**0,16**	**0,704**
LSL 1	10,2	10,22	**5,22**	**0,22**	**0,587**
LSL 1	10,26	10,28	**5,44**	**0,24**	**0,633**
LSL 1	10,32	10,34	**5,38**	**0,20**	**0,629**
LSL 1	10,38	10,4	**4,95**	**0,14**	**0,439**
LSL 1	10,44	10,46	**5,48**	**0,20**	**0,489**
LSL 1	10,5	10,52	**5,30**	**0,15**	**0,548**
LSL 1	10,56	10,58	**4,98**	**0,17**	**0,533**
LSL 1	10,62	10,64	**5,17**	**0,13**	**0,471**

LSL 1	10,68	10,7	**5,81**	**0,23**	**0,480**
LSL 1	10,74	10,76	**5,87**	**0,19**	**0,531**
LSL 1	10,8	10,82	**6,14**	**0,17**	**0,372**
LSL 1	10,86	10,88	**5,69**	**0,20**	**0,284**
LSL 1	10,92	10,94	**5,52**	**0,18**	**0,436**
LSL 1	10,98	11	**5,53**	**0,16**	**0,396**
LSL 1	11,04	11,06	**5,26**	**0,15**	**0,386**
LSL 1	11,1	11,12	**5,00**	**0,14**	**0,402**
LSL 1	11,16	11,18	**5,03**	**0,17**	**0,421**
LSL 1	11,22	11,24	**4,43**	**0,12**	**0,594**
LSL 1	11,28	11,3	**4,21**	**0,02**	**0,519**
LSL 1	11,34	11,36	**4,34**	**0,02**	**0,429**
LSL 1	11,4	11,42	**3,93**	**0,02**	**0,489**
LSL 1	11,46	11,48	**4,09**	**0,02**	**0,245**
LSL 1	11,52	11,54	**4,73**	**0,02**	**0,166**
LSL 1	11,58	11,6	**4,43**	**0,01**	**0,102**

Anleitung zur makroskopischen Beschreibung von Bohrkernen im Gelände

Martin Kehl
Universität zu Köln, Geographisches Institut

In der Fassung vom 1.10.2010

Anleitungen zur makroskopischen Beschreibung des Bohrkerns

1. Laufende Nr. der Lage

Zur Abgrenzung von Sedimentlagen (=sedimentäre Schichten und Bodenhorizonte)

Vor der Aufnahme wird der Kern mit dem Kittmesser gereinigt und quer zur Vortriebrichtung geglättet. Nach dem ersten Gesamteindruck - insbesondere unter Berücksichtigung der Farbe, Fleckung und Körnung - wird eine Unterteilung des Kernabschnittes in Lagen vorgenommen. Während der anschließenden Inventur der im Aufnahmeprotokoll zusammengestellten Sedimentmerkmale kann ggf. noch eine Revision der Lagenabgrenzung vorgenommen werden.

2. Untergrenze

Die Untergrenzen der Lagen werden mit Tiefe unter Geländeoberfläche und Art des Übergangs (Tab. 1) festgehalten.

Tab. 1: Beschreibung der Art des Übergangs an Untergrenzen von Lagen

Art des Übergangs	Code	Innerhalb
Scharf	S	0-1 cm
Deutlich	De	1-3 cm
Allmählich	A	3-6 cm
Diffus	Di	> 6 cm

3. Farbe

Die Farbbestimmung kann durch Vergleich mit MUNSELL-Farbtafeln möglichst exakt und reproduzierbar vorgenommen werden. Dabei sind **im feuchten Zustand** des Sediments folgende Farbkomponenten zu bestimmen:

Farbton – Hue

Entspricht bestimmten Ausschnitten aus dem sichtbaren Farbspektrum bzw. den Seiten der Tafel.

Farbhelligkeit - Value

Entspricht Gesamtintensität der Reflexion (Höhe des Schwarz- und Weißanteils) bzw. den Zeilen jeder Farbtafel-Seite.

Farbtiefe - Chroma

Entspricht der Breite des Ausschnittes bzw. Spalten jeder Farbtafel-Seite.

Der vollständige Code einer Farbbestimmung ist bspw. 7.5YR 3/4 oder 10YR 5/3.

4. Fleckung, Bänderung

Flecken gehen z.B. aus der Umverteilung von Fe- und Mn-Hydroxiden, Carbonaten und organischer Substanz hervor und können wichtige Hinweise auf die Veränderung des Sediments durch Prozesse der Bodenbildung geben. Zudem können sie die Lage des aktuellen oder ehemaligen Grundwasserschwankungsbereichs sowie von Stauwasserhorizonten anzeigen.

Die Flecken werden näherungsweise nach Flächenanteil und Größe erfasst:

Tab. 2: Flächenanteil der Flecken

Code	Beschreibung	%
K	Keine	0
S	Sehr wenige	< 2
W	Wenige	2-10
V	Viele	10-30
SV	Sehr viele	> 30

Tab. 3: Größe der Flecken

Code	Beschreibung	Mm
SF	Sehr fein	< 2
F	Fein	2-6
MG	Mittelgroß	6-20
G	Groß	> 20

5. Feuchte

Die aktuelle Feuchte wird grob nach **trocken, feucht, nass** und **wassergesättigt** differenziert. Dazu von unten leicht gegen die Kernsonde klopfen. Bei Wassersättigung tritt Wasser an der Oberfläche des gesäuberten Kerns auf.

6. Bodenart

Die in Sedimenten und Böden vorkommenden Korngrößen werden folgenden Größenklassen zugeordnet:

Tab. 4: Korngrößenfraktionen des Feinbodens (∅ unter 2 mm)

Fraktion (µm)	2000 – 63 Sand (S)	63 – 2 Schluff (U)	< 2 Ton (T)
Grob-	2000 - 630 gS	63 – 20 gU	2,0 - 0,63 gT
Mittel-	630 - 200 mS	20 - 6,3 mU	0,63 - 0,20 mT
Fein-	200 - 63 fS	6,3 – 2 fU	< 0,20 fT

Für die Definition der einzelnen **Bodenarten** des Feinbodens sind die Fraktionen Ton (T), Schluff (U) und Sand (S) maßgebend. Nach dem Vorherrschen einzelner Fraktionen werden die Bodenartenhauptgruppen der **Sande**, **Schluffe** und **Tone** unterschieden. Eine weitere Hauptgruppe bilden die **Lehme**, die in ihren Eigenschaften zwischen den erstgenannten Hauptgruppen stehen. Die Bodenartenhauptgruppen und -untergruppen (adjekt. Zusatz von s=sandig, l=lehmig, u=schluffig, t=tonig) werden in Form eines Dreiecksdiagramms (s. Abb. 1) oder tabellarisch dargestellt. Die **Körnung** des Feinbodens (Partikel < 2 mm) wird im Gelände mit der **Fingerprobe** ermittelt:

Hierzu Bodenprobe gleichmäßig knetend so weit befeuchten, dass kein Wasserglanz zu erkennen ist. Anschließend zwischen Daumen und Zeigefinger und durch Rollen im Handteller Bindigkeit, Formbarkeit und Körnigkeit prüfen. Die Schätzung der Bodenarten erfolgt nach den Hauptmerkmalen der verschiedenen Kornfraktionen:

Tone: glänzende Reibfläche, sehr gut formbar, plastisch.
Lehme: formbar, bleistiftdick rollbar, stumpfe bis glänzende Reibflächen.
Schluffe: mehlig, wenig formbar, Feinsubstanz haftet in den Fingerrillen .
Sande: Einzelkörner sicht- und fühlbar, nicht formbar.

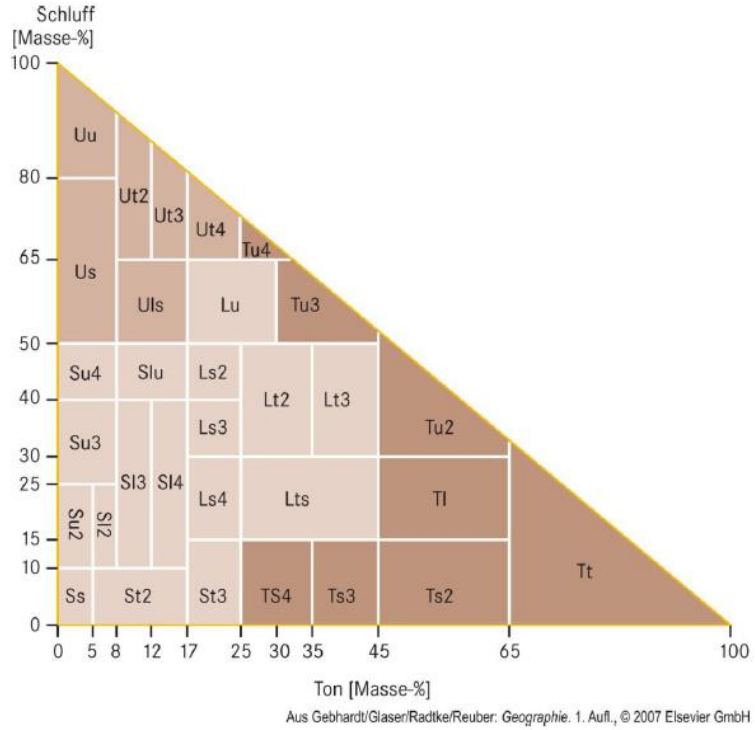

Abb. 1: Bodenartendreieck nach bodenkundlicher Kartieranleitung (Ad-hoc AG Boden 2005)

Tab. 5: Kriterien zum Schätzen der Bodenart mit der Fingerprobe

Kriterium Bindigkeit		
Stufe	Zusammenhalt der Probe	Zerbröckelt/zerbröselt/zerbricht
0	Kein	Sofort
1	Sehr gering	Sehr leicht
2	Gering	Leicht
3	Mittel	Wenig
4	Stark	Kaum
5	Sehr stark	Nicht

Kriterium Formbarkeit (Ausrollbarkeit[1])	
0	Nicht ausrollbar, zerbröckelt beim Versuch
1	Nicht ausrollbar, da die Probe vorher reißt und bricht
2	Ausrollen schwierig, da die Probe starke Neigung zum Reißen und Brechen aufweist
3	Ohne größere Schwierigkeiten ausrollbar, da die Probe nur schwach reißt oder bricht
4	Leicht ausrollbar, da die Probe nicht reißt oder bricht
5	Auf dünner als halbe Bleistiftstärke ausrollbar

[1] Bewertung der Formbarkeit und Ausrollbarkeit einer Probe auf halbe Bleistiftstärke

Tab. 6: Bestimmungsschlüssel (FS = Feinsubstanz, hier Schluff und Ton)

Hauptgruppe	Gruppe	Bodenart	Bindigkeit	Formbarkeit	Körnigkeit	Weitere Erkennungsmerkmale
Sande	**Reinsande**	Ss	0	0	Nur Sandkörner, ohne erkennbare FS	In Fingerrillen haftet keine oder kaum FS
	Lehmsande	Su2	0	0	Sandkörner gut sicht- und fühlbar, sehr wenig FS	In Fingerrillen haftet sehr wenig FS
		Sl2	1	1-2	Sandkörner deutlich sicht- und fühlbar, sehr wenig FS	In Fingerrillen haftet wenig FS
		Sl3	2	3	Sandkörner deutlich sicht- und fühlbar, sehr wenig bis mäßig FS	In Fingerrillen haftet FS
		St2	1-2	1-3	Sandkörner sicht- und fühlbar, sehr wenig FS	In Fingerrillen haftet sehr wenig FS
	Schluffsande	Su3	0-1	0-2	Sandkörner gut sicht- und fühlbar, deutlich FS führend	In Fingerrillen haftet schwach mehlige FS
		Su4	0-1	0-2	Sandkörner gut sicht- und fühlbar,viel FS	In Fingerrillen haftet stark mehlige FS
Lehme	**Sandlehme**	Slu	1-2	3	Sandkörner deutlich sicht- und fühlbar,viel FS	FS ist deutlich mehlig
		Sl4	2	3	Sandkörner gut sicht- und fühlbar, mäßig bis viel FS	Schwach glänzende Reibfläche, walnussgroße Kugel formbar
		St3	3	3	Sandkörner deutlich sicht- und fühlbar, mäßig FS führend	Sehr klebrige FS („Honigsand“)
	Normallehme	Ls2	3	3	Sandkörner deutlich sicht- und fühlbar, viel FS	Sehr schwach mehlige FS
		Ls3	3	3	Sandkörner deutlich sicht- und fühlbar, viel FS	Glänzende Reibfläche, sehr deutlich körnig
		Ls4	3	3	Sandkörner deutlich sicht- und fühlbar, mäßig FS führend	Schwach glänzende Reibfläche, sehr deutlich körnig
		Lt2	4	4	Sandkörner gut sicht- und fühlbar, sehr viel FS	Schwach raue, schwach glänzende Reibfläche
	Tonlehme	Lts	4-5	4-5	Sandkörner gut sicht- und fühlbar, reich an FS	Sehr stark glänzende Reibfläche, körnig

		Ts4	4	4	Sandkörner gut sicht- und fühlbar, viel FS	Raue, glänzende Reibfläche, deutlich körnig
		Ts3	5	5	Sandkörner deutlich sicht- und fühlbar, sehr viel FS	Schwach raue, glänzende Reibfläche, deutlich körnig, klebrig, zähplastisch
Schluffe	**Sand-schluffe**	Uu	0-1	1	Sandkörner kaum oder nicht sicht- und fühlbar, fast nur FS	Samtig-mehlige FS haftet deutlich in Fingerrillen, Reibfläche matt u. auf-schuppend
		Us	0-1	1	Sandkörner sicht- und fühlbar, FS überwiegt	Samtig-mehlige FS haftet deutlich in Fingerrillen, Reibfläche körning, matt u. aufschuppend
	Lehm-schluffe	Ut2	1	2	Sandkörner kaum oder nicht sicht- und fühlbar, fast nur FS	Stark mehlige FS haftet deutl. in Fingerrillen, raue, matte und aufschuppende Reibfläche
		Ut3	2	2	Sandkörner nicht sicht- und fühlbar, fast nur FS	deutlich mehlige FS haftet gut in Fingerrillen, Reibfläche matt und aufschup-pend
		Uls	1-2	1-3	Sandkörner sicht- und fühlbar, FS überwiegt	Leicht mehlige FS haftet deutl. in Fingerrillen
	Ton-schluffe	Ut4	3	3	Sandkörner nicht sicht- und fühlbar, nur FS	Schwach mehlige FS haftet und klebt etwas, matte bis schwach glänzende Reibfläche, körnig und aufschup-pend
		Lu	3-4	3-4	Sandkörner nicht oder kaum sicht- und fühlbar, sehr viel FS	Bindige FS, raue, matte bis schwach glänzende Reibfläche, körnig u. aufschup-pend
Tone	**Schluff-tone**	Lt3	5	5	Sandkörner sicht- und fühlbar, sehr viel FS	Zähplastische FS, schwach raue, schwach körnige, glänzende Reibfläche
		Tu3	4-5	5	Sandkörner nicht sicht- und fühlbar, fast nur FS	Zähplastische FS, schwach raue, glänzende Reibfläche
		Tu4	4	4	Sandkörner nicht sicht- und fühlbar, nur FS	Raue, schwach glänzende Reibfläche, knirscht zwischen den Zähnen
	Lehm-tone	Ts2	5	5	Wenig Sandkörner sicht- und fühlbar, reich an FS	Stark glänzende Reibfläche, knirscht zwischen den Zähnen
		Tl	5	5	Sehr wenig sandkörner sicht- und fühlbar, sehr viel FS	Zähplastische FS, glänzende Reibfläche
		Tu2	5	5	Sandkörner nicht sicht- und fühlbar, fast nur FS	Stark plastische FS, schwach raue, glänzende Reibfläche
		Tt	5	5	Sandkörner nicht sicht- und fühlbar, nur FS	Stark plastische, mm-dünn ausrollbare FS, glatte, schwach glänzende bis glänzende Reibfläche

Anmerkung: Die tonmineralogische Zusammensetzung kann die Ansprache beeinflussen. Smektitische Tonminerale sind sehr plastisch und Kaolinite kleben stark. Der Tongehalt kann bei ersteren überschätzt und bei letzteren unterschätzt werden.

Reine Sande werden nach der dominierenden Sandfraktion als Feinsande (fS: viel 0,06 - 0,2 mm ∅), Mittelsande (mS: viel 0,2 - 0,6 mm ∅) bzw. Grobsande (gS: viel 0,6 - 2 mm ∅) angesprochen.

Nebenfraktionen können durch nachgestellte Ziffer abgeschwächt (=2) oder verstärkt (=4) werden, z.B. Sl2 = schwach lehmiger Sand oder Ls4 = stark sandiger Lehm.

Die Bestimmung der Bodenart ist bei höheren Gehalten an organischer Substanz schwierig; die organische Substanz erhöht Bindigkeit und Formbarkeit, daher vor allem bei Sanden - je nach Humusgehalt - 1-2 Körnungsklassen zurückstufen.

7. Grobanteil

Es wird notiert, ob sich Kies oder Gruskörner (gerundete oder scharfkantige Partikel mit Korndurchmessern von mehr als 2 mm) im Bohrkern befinden. Diese Partikel geben Hinweisauf die Sedimentations- und Verwitterungsbedingungen. Falls möglich, sollte auch die Petrographie des Grobanteils angesprochen werden. Vorsicht ist beim Auftreten von Konkretionen aus Carbonaten, Eisenhydroxiden oder Gips geboten, die in der Spalte Konzentrationen vermerkt werden.

Tab. 7: Aufnahme des Skelettanteils

Skelettanteil Flächen-%	gerundet,	rund, 2 - 63 mm	kantig, 2 - 63 mm	Code
< 1	sehr schwach	kiesig (g)	grusig (gr)	1
1 - 10	schwach	〃	〃	2
10 - 30	mittel	〃	〃	3
30 - 50	stark	〃	〃	4
50 - 75	sehr stark	〃	〃	5
>75	Skelettboden	〃	〃	X, G, Gr

8. Carbonatgehalt

Der Carbonatgehalt kann grob nach Stärke und Dauer des Aufbrausens nach Behandlung mit Salzsäure (HCl 10 %) geschätzt werden (**Vorsicht!** Verursacht Verätzungen, bei Berührung mit viel Wasser spülen):

Tab. 8: Schätzen des Carbonatgehalts

Aufbrausen	Carbonate (%)	Bezeichnung	Code
Keine Reaktion	0	carbonatfrei	c0
sehr schwach (nur hörbar)	< 0,5	sehr carbonatarm	c1
Schwach	0,5 - 2	carbonatarm	c2
deutlich, nicht anhaltend	2 - 10	(mäßig) carbonathaltig	c3
stark anhaltend	10 - 25	carbonatreich	c4
sehr stark, lang anhaltend	> 25	sehr carbonatreich	c5

9. Organische Substanz

Der Gehalt der organischen Substanz (Humus) kann grob aus der an einer feuchten Probe bestimmten Bodenfarbe abgeschätzt werden, wobei allerdings die Körnung berücksichtigt werden muss.

Tab. 9: Schätzung des Humusgehalts auf Grundlage der Farbbestimmung und Bodenarten-Ansprache

Farbe	Munsell value	Sand	Lehmiger Sand, sandiger Lehm, Lehm	Alle übrigen
Hellgrau	7			
Hellgrau	6.5			
Grau	6			
Grau	5.5			< 0,3
Grau	5	< 0,3	< 0,4	0,3-0,6
Dunkelgrau	4.5	0,3-0,6	0,4-0,6	0,6-0,9
Dunkelgrau	4	0,6-0,9	0,6-1,0	0,9-1,5
Schwarzgrau	3.5	0,9-1,5	1-2	1,5-3,0
Schwarzgrau	3	1,5-3,0	2-4	3-5
Schwarz	2.5	3-6	>4	>5
Schwarz	2	>6		

Der Humusgehalt wird wie folgt eingestuft:

Masse-%	Bezeichnung	Kurzzeichen
0	humusfrei	h0
<1	sehr schwach humos	h1
1 bis <2	schwach humos	h2
2 bis <4	mittel humos	h3
4 bis <8	stark humos	h4
8 bis <15	sehr stark humos	h5
15 bis <30	extrem humos, anmoorig	h6
> 30	organisch, Torf	h7

10. Lagerung

Die Lagerungsdichte (d_B) beschreibt die Masse trockenen Sediments pro Volumeneinheit, die neben der Feuchte und Körnung den Eindringwiderstand beim Bohrvorgang bestimmt. Aufgrund von Sedimentstauchungen beim Bohren ist die Lagerungsdichte im Bohrkern nur grob abzuschätzen nach: gering (= L1), mittel (L2), hoch (L3) und sehr hoch (L4).

11. Konzentrationen

Die Anreicherung von Ton, Sekundärcarbonat oder Eisen- und Manganhydroxiden deutet auf Bodenbildung und/oder Anreicherung aus dem Grundwasser oder lateral ziehendem Hangwasser hin. Das Auftreten folgender Konzentrationen wird notiert:

- Tonbeläge nach Farbe und Menge
- Sekundärcarbonat: nach Art (weiche Konkretionen, harte Konkretionen, pulverförmig, Pseudomycelien, Mergellage, zementierte Kalkkruste) und Menge
- Gipskristalle ja oder nein
- Fe-und Mn-hydroxide: nach Härte (weich, hart), Größe (maximale Durchmesser in mm) und Art der Anreicherung (Konkretionen, Bänder, Adern, Krusten)

12. Bemerkungen

In dieser Spalte sollen alle Besonderheiten vermerkt werden. Dies sind z.B. Auftreten von Wurzeln, Verschleppung von Sediment, Kernverluste etc. Außerdem Benennung des Sedimenttyps.